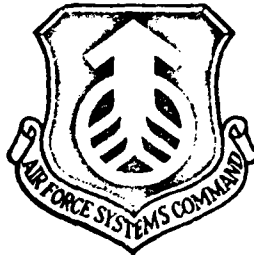


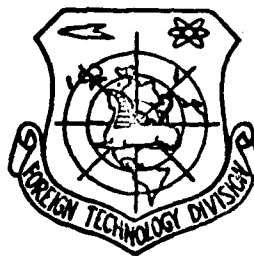
MICROCOPY RESOLUTION TEST CHART
NATIONAL BUREAU OF STANDARDS-1963-A₁

2
FW
FTD-ID(RS)T-0940-81

FOREIGN TECHNOLOGY DIVISION



ANTENNA
(Selected Articles)



DTIC
ELECTE
DEC 8 1981
A

Approved for public release;
distribution unlimited.

81 12 08 124

AD A108174

DTIC FILE COPY

EDITED TRANSLATION

FTD-ID(RS)T-0940-81 4 November 1981

MICROFICHE NR: FTD-81-C-001006

ANTENNA (Selected Articles)

English pages: 59

Source: Antenny, Nr. 15, 1972, pp. 31-79

Country of origin: USSR

Translated by: SCITRAN

F33657-81-D-0263

Requester: FTD/TQFE

Approved for public release; distribution unlimited.

THIS TRANSLATION IS A RENDITION OF THE ORIGINAL FOREIGN TEXT WITHOUT ANY ANALYTICAL OR EDITORIAL COMMENT. STATEMENTS OR THEORIES ADVOCATED OR IMPLIED ARE THOSE OF THE SOURCE AND DO NOT NECESSARILY REFLECT THE POSITION OR OPINION OF THE FOREIGN TECHNOLOGY DIVISION.

PREPARED BY:

TRANSLATION DIVISION
FOREIGN TECHNOLOGY DIVISION
WP-AFB, OHIO.

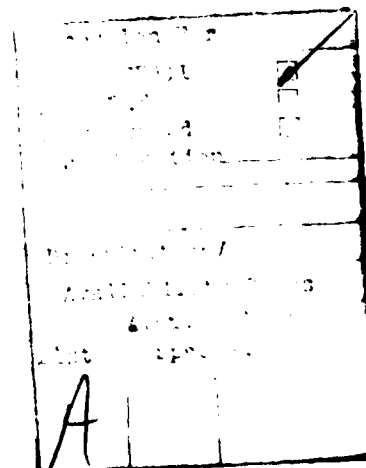
FTD-ID(RS)T-0940-81

Date 4 Nov 19 81

14610

TABLE OF CONTENTS

U. S. Board on Geographic Names Transliteration System....	11
Decreasing DG and Direction Dispersion of Main Maximum of Beam Pattern of Sectional Traveling Wave Antenna, by V. I. Zamyatin and L. G. Korniyenko.....	1
Statistics of the Field of Focused Systems, by A. S. Yevseyev.....	18
Efficiency and Input Impedance of Planar Emitter Placed Near the Interface, by V. P. Kul'tsep.....	30
Analysis of the Properties of Connected Vibrator Structures, by N. A. Bey and N. M. Yakusheva.....	45
Assessment of Aircraft Capacitive Circuit Medium Wave Antennas According to Their Efficiency, by E. O. Brudnyy and L. Ya. Il'nitskiy.....	53



U. S. BOARD ON GEOGRAPHIC NAMES TRANSLITERATION SYSTEM

Block	Italic	Transliteration	Block	Italic	Transliteration
А а	<i>А а</i>	A, a	Р р	<i>Р р</i>	R, r
Б б	<i>Б б</i>	B, b	С с	<i>С с</i>	S, s
В в	<i>В в</i>	V, v	Т т	<i>Т т</i>	T, t
Г г	<i>Г г</i>	G, g	У у	<i>У у</i>	U, u
Д д	<i>Д д</i>	D, d	Ф ф	<i>Ф ф</i>	F, f
Е е	<i>Е е</i>	Ye, ye; E, e*	Х х	<i>Х х</i>	Kh, kh
Ж ж	<i>Ж ж</i>	Zh, zh	Ц ц	<i>Ц ц</i>	Ts, ts
З з	<i>З з</i>	Z, z	Ч ч	<i>Ч ч</i>	Ch, ch
И и	<i>И и</i>	I, i	Ш ш	<i>Ш ш</i>	Sh, sh
Й й	<i>Й й</i>	Y, y	Щ щ	<i>Щ щ</i>	Shch, shch
К к	<i>К к</i>	K, k	Ъ ъ	<i>Ъ ъ</i>	"
Л л	<i>Л л</i>	L, l	Ы ы	<i>Ы ы</i>	Y, y
М м	<i>М м</i>	M, m	Ь ь	<i>Ь ь</i>	'
Н н	<i>Н н</i>	N, n	Э э	<i>Э э</i>	E, e
О о	<i>О о</i>	O, o	Ю ю	<i>Ю ю</i>	Yu, yu
П п	<i>П п</i>	P, p	Я я	<i>Я я</i>	Ya, ya

*ye initially, after vowels, and after ъ, ь; e elsewhere.
When written as ё in Russian, transliterate as yë or ë.

RUSSIAN AND ENGLISH TRIGONOMETRIC FUNCTIONS

Russian	English	Russian	English	Russian	English
sin	sin	sh	sinh	arc sh	sinh ⁻¹
cos	cos	ch	cosh	arc ch	cosh ⁻¹
tg	tan	th	tanh	arc th	tanh ⁻¹
ctg	cot	cth	coth	arc cth	coth ⁻¹
sec	sec	sch	sech	arc sch	sech ⁻¹
cosec	csc	csch	csch	arc csch	csch ⁻¹

Russian English

rot curl
lg log

DECREASING DG AND DIRECTION DISPERSION
OF MAIN MAXIMUM OF BEAM PATTERN OF
SECTIONAL TRAVELING WAVE ANTENNA

V. I. Zamyatin and L. G. Korniyenko

Summary

Formulas are found and analyzed to reduce the directive gain and direction dispersion of the main maximum of the beam pattern of a sectional traveling wave antenna when there are errors of the wave number in the system and phase errors at the sites of contact between the sections. A condition of optimality of sectioning and a condition in which the limiting directive gain is missing are obtained. The effectiveness of the sampling of phase errors is studied.

Introduction

Production conditions force us to assemble large antennas made of individual sections.

Since the dimensions of the sections are generally small, there is a possibility, first of all, of manufacturing them fairly accurately, and secondly, of setting up comparatively simply the measurement of the amplitude-phase distribution (APD) in the aperture of the sections and its deviation from the calculated value (errors).

The latter circumstance permits a more rational approach to assembly of the antenna, that is, use of the methods of assembly (sectional) which reduce the effect of random errors in APD on the antenna parameters.

A number of works have covered a statistical analysis of sectional antennas [1-3].

Publication [1] has studied the statistics of the field of inphase sectional antennas. Publications [2-3] have investigated the characteristics of linear [2] and two-dimensional [3] sectional traveling wave antennas (STWA) with different methods of sectioning.

Publication [2] in particular, has examined the STWA characteristics with random and selective methods of assembly. It has introduced an important parameter which characterizes the economic efficiency of production. Publication [3] has found the average beam pattern of the system which consists of a set of linear STWA with random and one-sided method of assembly, with sampling of errors at the end of each section.

One of the main results of these works is the conclusion that with an increase in the number of sections, the distortions of the beam pattern (BP) in antenna N diminish. This conclusion is correct in the case where the junction sites of the sections are ideal. In real antennas, at the junction sites, inhomogeneities naturally arise which result in random errors in the APD. In this case, enlargement of N results, on the one hand, in a decrease in errors governed by fluctuations in the wave number, and on the other hand, in an increase in the errors associated with the nonideal nature of the junctions. The same situation develops when the errors at the end of each section are not sampled completely, but with a certain error.

In these cases, a certain optimal solution evidently exists in selecting the number of sections.

In addition, the sampling of phase errors to zero at the end of each section which is examined in [3] can be difficult. It is therefore important to study a more general case where the error sampling is made only through M sections.

This work studies the statistics of STWA with the same methods of sectioning as in [2], but first of all, with sampling of the phase errors to zero through M sections, and secondly, with consideration for the phase errors which develop at the sites of the section junctions. For convenience, the same letter designations are adopted as in [2].

Initial Correlations

Assume that a STWA of length L is formed of N sections equal to length $l = \frac{L}{N}$ taken from the original group of sections.

When the antenna has phase errors, separate realization of the beam pattern for output looks like:

$$F(u, \sigma) = \left| \frac{1}{2} \sum_{n=1}^N e^{i \frac{\pi}{N} (2n-1)} \int_{-1}^1 A_n(y) e^{i \frac{\pi}{N} y + i \sigma \Phi_n(y)} dy \right|, \quad (1)$$

where $A_n(y)$ -- amplitude distribution in n-th section of STWA,

$\Phi_n(y) = \frac{\Delta \Phi_n(y)}{\sigma}$ -- fluctuations in the phase in the n-th section, classified as a certain quadratic value σ ,

$u = \frac{L}{2}(k_0 - k \cos \theta)$ -- generalized angle,

k, k_0 -- wave numbers in system and in free space respectively.

For simplicity, we will consider that the amplitude distribution in the antenna aperture is uniform, and the phase velocity of the wave in the system is greater than or equal to the speed of light. Then, in the absence of errors, the direction of the main maximum $u_0 = 0$ and the beam pattern $F(u, 0) = L^2 \frac{\sin^2 u}{u^2}$. When there are small phase errors, the directional drift of the main maximum Δu is determined by the ratio (A.3) with $b = \sigma$ and $A_u = \frac{\partial}{\partial u}$ and equals¹):

¹In publication [2], the correlation for the directional drift of the main BP maximum is presented in relation to $\psi = \frac{u}{N} = 1/2 (k_0 - k \cos \theta)$. For the purposes of this work, recording in relation to u is preferable since in the majority of cases the length of the antenna is considered constant.

$$\Delta u = -\frac{\sigma^2}{4NF_{\text{om}}(0, 0)} \sum_{n, m=1}^N \int_{-1}^1 \int_{-1}^1 [2(n-m) + y - y_1] \times \\ \times [\Phi_n(y) - \Phi_m(y_1)] dy dy_1 = -\frac{3\sigma}{2N^3} \sum_{n=1}^N \int_{-1}^1 [2n + y - N - 1] \Phi_n(y) dy. \quad (2)$$

Then the decrease in dg (directive gain)

$$\Delta = 1 - \frac{F(0, \sigma)}{F(0, 0)} \approx 1 - \frac{\sigma^2}{2L^3} \overline{F_{\text{od}}''(0, 0)}. \quad (3)$$

It is considered in (3) that $\overline{F_{\text{od}}''(0, 0)} = 0$. The line above designates the operation of averaging for the group of realizations.

As is apparent from (1,2,3), for further computations it is necessary to know the statistical characteristics of phase fluctuations in the antenna.

Statistics of Phase Fluctuations in the STWA

Assume that the technology for fabricating the original group of sections is such that the wave number in each section differs from the theoretical k by a random quantity Δk . Then the fluctuations in the phase in the n -th section of the formed STWA are described by the expression

$$\Phi_n(y) = l \sum_{i=1}^{n-1} \delta \kappa_i + 0.5 \delta \kappa_n l(y+1) + \sum_{i=1}^{n-1} \delta \gamma_i, \quad (4)$$

where $\delta \kappa_i = \frac{\Delta \kappa_i}{\sigma}$ --fluctuations in wave number in i -th section of formed STWA classified as the quantity σ
 $\delta \gamma_i = \frac{\Delta \gamma_i}{\sigma}$ --phase error at end of i -th section governed by imperfection in the section junctions, and also classified as the quantity σ .

Separate realization of the phase fluctuations in distribution is shown in fig. 1a.

It follows from (4) that the total errors $\Phi_n(y)$ increase with the number of the section, i.e., the quantity of the phase error in the n -th section is significantly affected by the phase errors in the previous sections.

We assume that the average value $\overline{\Delta \gamma_i} = 0$, then

$$\overline{\Delta \kappa_i \Delta \gamma_j} = 0, \quad \overline{\Delta \gamma_i \Delta \gamma_j} = \begin{cases} 0, & i \neq j, \\ \sigma_\gamma^2, & i = j. \end{cases} \quad (5)$$

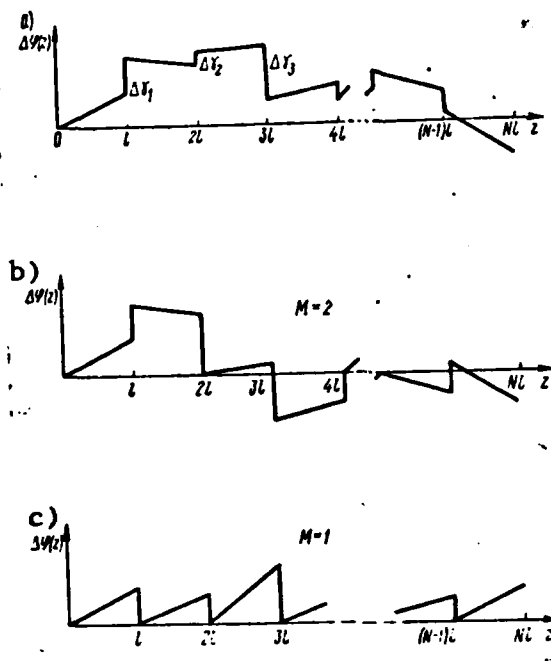


Figure 1.

The statistical characteristics $\Delta \kappa_i$ depend on the statistics of the wave number of the original group of sections, methods of rejection and sectioning.

Assume that the wave number of the original group of sections is distributed according to the normal law with zero average value $\Delta k=0$ and dispersion σ_0^2 .

We will consider the sections suitable for assembly of the antenna if the phase incursion on the length of the section (equal to $\Delta k l$) does not exceed the tolerance a , i.e., $|\Delta k l| \leq a$. The sections that do not satisfy this condition are rejected.

With the selected method of rejection, the wave number of the "working" group of sections is subordinate to a limited normal law of

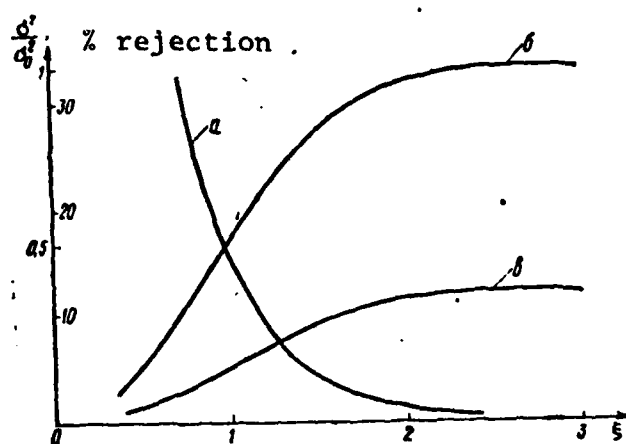


Figure 2.

distribution:

$$W(x) = \begin{cases} \frac{\exp\left(-\frac{x^2}{2\sigma_0^2}\right)}{\sigma_0 \sqrt{2\pi} \phi(\xi)}, & |x| \leq \frac{a}{l}, \\ 0, & |x| > \frac{a}{l}, \end{cases} \quad (6)$$

where $\phi(\xi) = \frac{2}{\sqrt{\pi}} \int_0^\xi e^{-t^2} dt$ --- integral of probability,
 $\xi = \frac{a}{\sqrt{2}\sigma_0 l}$ --- parameter associated with the percentage of section rejection.

Thus, for example, 1% rejection corresponds to the probability $p(|x| \leq \frac{a}{l}) = \phi(\xi) = 0.99$, from which $\xi = 1.83$.

The dependence of the percentage of rejection on ξ is graphically presented in fig. 2 (curve a). It is apparent from the figure that the smaller values of rejection percentage correspond to the larger ξ , and with $\xi \gtrsim 2$, the percentage of rejection changes slightly and the rejection of sections may not be done. Since ξ is unequivocally linked to the percentage of rejection, the quantity ξ characterizes the degree of economy of production.

We will now examine the effect of the sectioning methods on the statistic of the average number. For this purpose we will examine the selective (I method) and random (II method) layouts of the antenna from

the "working" group of sections [2]. With random arrangement, the sections of the working group are selected according to the following law. In this case, the wave number in the i -th section of the STWA will evidently be distributed according to the limited normal law (6).

With selective arrangement, sections are installed in the first place in the antenna with positive phase incursion $\Delta k_1 > 0$, the second place, with negative incursion $\Delta k_1 < 0$, etc. With this method of sectioning, the wave number in the i -th section of the formed TWA is distributed according to the limited one-sided normal law.

By knowing the laws of distribution, it is easy to obtain expressions for the average value $\overline{\Delta k_i}$ and dispersion σ^2 of the wave number in the i -th section of the STWA. These expressions are presented in [2]. Here we will only note that for the I method, $\overline{\Delta k_i}$ is constant for each section, positive in the odd, and negative in the even sections, and for the II method $\overline{\Delta k_i} = 0$. Dispersion σ^2 does not depend on the number of the section and is determined by the dispersion of the original group of sections σ_0^2 and the parameter of rejection ξ . The dependence of σ^2/σ_0^2 on this parameter for both methods of assembly is presented in fig. 2 (curves b and c respectively). The expediency of using the I method of sectioning is apparent from the figure, since in this case, σ^2 is roughly three times smaller than in the II method.

Decrease in DG, Directional Dispersion of the Main Maximum

Using different design measures, we will "sample" the phase error in the antenna aperture to zero through M sections (fig. 1b). For simplicity we assume that the TWA consists of a whole number of groups of M sections each, i.e., $N = \omega M$. Then the correlations for $F(0, \sigma)$ and Δu look like:

$$F(0, \sigma) = \frac{1}{4} \left| \sum_{v=1}^{\omega} \sum_{p=1}^M \int_{-1}^1 e^{i\sigma \phi_{p+(v-1)M}(y)} dy \right|^2, \quad (7)$$

$$\Delta u = -\frac{3\sigma}{3N^2} \sum_{v=1}^{\omega} \sum_{p=1}^M \int_{-1}^1 [2(p+vM-M) + y - N - 1] \phi_{p+(v-1)M}(y) dy. \quad (8)$$

Since errors at the end of each group are sampled to zero and in each group the same algorithms are used for installing sections made

of a "working" group of large volume, then, evidently, the phase fluctuations in each group are statistically equivalent and independent of each other.

This makes it possible to consider that

$$\overline{\Phi_{p+(v-1)M}^0(y) \Phi_{q+(\mu-1)M}^0(y_1)} = \begin{cases} \overline{\Phi_p^0(y) \Phi_q^0(y_1)}, & v = \mu, \\ 0, & v \neq \mu, \end{cases} \quad (9)$$

where Φ_0 designates the centered quantities. The calculations of the amount of decrease in dg according to formula (3) with regard for ratio (7), the average value and dispersion of the course of direction of the main maximum using formula (8) are fairly cumbersome, however do not involve any basic difficulties. In the computations, it is first of all necessary to take into consideration ratio (9), then ratios (4) and (5), and also to additionally hypothesize that the correlation coefficient (with $i \neq j$) of the fluctuations in the wave number Δk_i equal zero.

Taking into consideration the equality $\sum_{p < q}^M = \sum_{p=1}^{M-1} \sum_{q=p+1}^M = \sum_{q=2}^M \sum_{p=1}^{q-1}$,

after the appropriate computations, we can write the following final results:

1) decrease in dg with sampling of the phase error to zero through M sections

$$\Delta_M = \frac{1}{12N} (M-1) (6N-4M+2) \left(\sigma_v^2 + \frac{\sigma^2 L^2}{N^2} \right) - \frac{\sigma^2 L^2}{12N^2} \left[(6M-4N-3) - (4N-3M) \frac{|\Delta \bar{\kappa}_L|^2}{\sigma^2} \right]; \quad (10)$$

2) average direction of main maximum

$$\overline{\Delta u} = -a_M \frac{|\Delta \bar{\kappa}_L| L}{2MN^2}, \quad (11)$$

where $a_M = \begin{cases} 0 & \text{with } M \text{ even,} \\ 1 & \text{with } M \text{ odd;} \end{cases}$

3) dispersion of the direction of the main maximum of the BP

$$\sigma_{uM}^2 = \frac{1}{10N^2} \left[M^2 (10\omega^2 - 7) \left(\frac{\sigma^2 L^2}{N^2} + \sigma_v^2 \right) - \frac{\sigma^2 L^2}{2N^2} (5N^2 - 4) - \sigma_v^2 [5M^2 (\omega^2 - 1) (3M - 1) + 3] \right]. \quad (12)$$

Analysis of Results

We initially will analyze the effect on the quantities Δ_M , $\overline{\Delta u}$, $\sigma_{\Delta u}^2$ of the errors in wave number Δk_i and phase errors at the end of the sections $\Delta \gamma_i$ in the absence of sampling of the total phase error $\phi_n(y)$. We will then evaluate the effect on the indicated parameters of a sampling with $\sigma_\gamma^2 = 0$, and finally, we will examine a general case where sampling of errors through M sections is stipulated in the antenna and errors Δk_i and $\Delta \gamma_i$ are present. We will examine several possible situations.

1. Sampling of the phase error is not done ($M=N$, $\omega=1$). In this case, with $\sigma_\gamma^2=0$, the ratios for Δ_N , $\overline{\Delta u}$ and σ_{uN}^2 have been analyzed in publication [2]. It is noted there, that both for I and for II methods of sectioning, with $\sigma L = \text{const}$, distortions in the beam pattern are reduced with an increase in the number of sections. This result is almost obvious, since with an increase in the number of sections with $L = \text{const}$, dispersion of the phase errors diminishes. When there are errors which arise at the sites of junction of the sections, the situation changes: increase in the number of sections, on the one hand results in a decrease in the dispersion of phase errors governed by fluctuations in the wave number, and on the other hand, in an increase in the phase errors over the length of the antenna which are governed by inhomogeneities at the sites of section contact.¹

A similar situation must result in the presence of certain values N at which ΔN and σ_{uN}^2 will be the minimum, i.e., in the existence of an optimal number of sections from which the STWA is assembled. With fairly large N, where in formulas (10) and (12) with $M=N$ and $\omega=1$, one can ignore the terms of a higher order of smallness than $1/N$, the minimum values for decrease in dg and dispersion of direction of the main BP maximum are reached practically simultaneously with

$$N \approx \frac{1}{\alpha}, \quad (13)$$

¹By using (4), it is easy to show that the maximum dispersion of the total phase errors is reached at the end of the antenna and equals:
 $\sigma_{\phi N}^2 = \frac{\sigma^2 L^2}{N} + (N-1)\sigma_\gamma^2$. The first term is associated with errors in the wave number, while the second is associated with phase errors at the sites of junction of the sections.

where $\alpha = \frac{\sigma_Y}{\sigma_L}$ --ratio of standard value of phase error at the sites of junction of the sections to the standard phase incursion at length L in the presence of fluctuations in the phase of the wave number. Since ratio (13) was obtained on the hypothesis that $N \gg 1$, then when it is used, the condition $\sigma L \gg \sigma_Y$ must be fulfilled.

When this condition is fulfilled (in addition to the condition for smallness of the errors $\sigma_{\phi N}^2$ (see the footnote on p. 00 [sic]) in which the correlations (10 and (12) were obtained, from formula (13) one can determine the number of sections into which the antenna needs to be "divided" in order to obtain the minimum distortions of the beam pattern.

Since the quantity σ^2 during selective layout is smaller than during random layout, then the STWA can be formed from a smaller number of sections.

The dependence of the parameters $\frac{\Delta_N}{\sigma^2 L^2}$ and $\frac{\sigma_{uN}^2}{\sigma^2 L^2}$ on the number of sections N with different values of α is presented in figs. 3 and 4. Figure 3 illustrates the dependence of the ratio $\frac{\Delta_Y}{\sigma^2 L^2}$ on the number of sections with random layout of the antenna (i.e. $|\Delta \kappa_i| = 0$).

It is apparent from the figure that in the region of optimal N , the quantities Δ_N and σ_{uN}^2 change slowly. With $\alpha=0$, the optimums are missing and the distortions of the beam pattern are smaller, the greater the number of sections N .

Above we examined a case where the length of an antenna made of a different number of sections remained constant, while the length of the sections changed $l=L/N$. When the antenna is assembled from sections of a fixed size ($l=\text{const}$), the increase in N results in an increase in errors governed both by fluctuations in the wave number Δk_i and by phase errors at the sites of junction $\Delta \gamma_i$. In this case, the distortions in the beam pattern increase: Δ_N increases, and the dispersion of the direction of the main BP maximum rises.

2. A sampling is made in every other M section of the phase errors ($M = \frac{N}{\omega}$), errors at the sites of junction are missing ($\sigma_Y^2 = 0$). In this case we study the effect of the "frequency" of sampling the errors on the STWA characteristics. For this purpose, we analyze expressions (10), (11) and (12) with $\sigma_Y^2 = 0$.

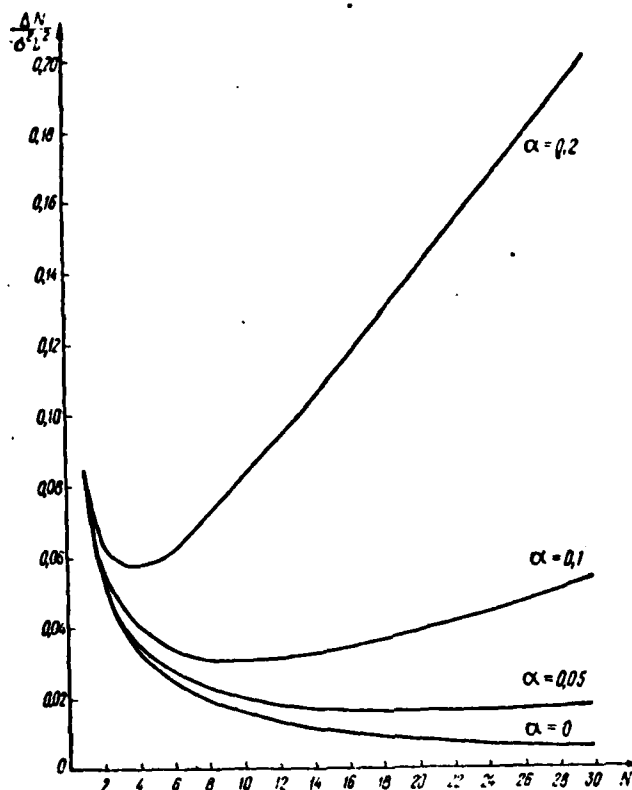


Figure 3.

We will first examine the average value and dispersion of the direction of the main BP maximum.

With random layout of the sections and (or) an even number of sections in the group, the direction of the main BP maximum is maintained on the average the same as in the absence of errors. When errors are sampled after each section, the quantity $\overline{\Delta u}$ is the maximum. With an increase in the number of sections in the antenna (with $L = \text{const}$) or in the group in the I method of assembly, $\overline{\Delta u}$ is diminished. These relationships have a simple physical interpretation, if we examine the phase distribution in the group of sections. Thus, for example, with $M=1$ and the I method of assembly, the distribution of phase errors in the antenna is shown in fig. 1c, and the average distribution of errors is the same. Evidently, $\overline{\Delta u}$ in this case will be the maximum.

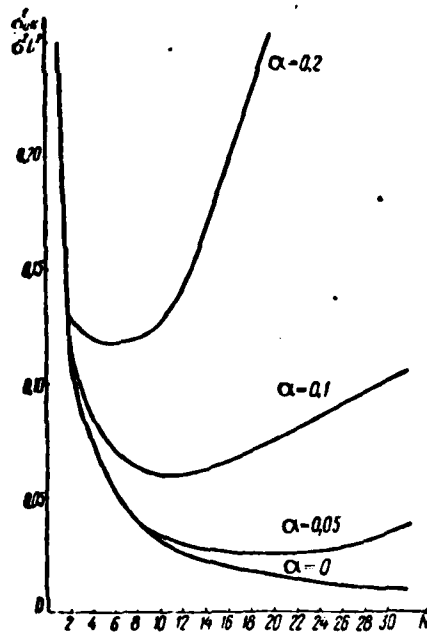


Figure 4.

For simplicity, we will introduce the following quantity into the examination

$$\kappa_u = \frac{\sigma_{uN}^2}{\sigma_{uM}^2},$$

where $\sigma_{uN}^2, \sigma_{uM}^2$ --dispersions of direction in the main BP maximum of the antenna without sampling of the phase errors and antenna with sampling of the errors in M sections respectively. For the examined case, the quantity σ_{uN}^2 is determined by the correlation (12) with $N=M$ and $\sigma_y^2 = 0$, and is analyzed in fair detail, as previously noted, in publication [2]. Since $\sigma_{uN}^2 \geq \sigma_{uM}^2$, then the expression $\kappa_u = \sigma_{uN}^2 / \sigma_{uM}^2$ characterizes the gain in dispersion of the direction of the main maximum because of sampling the phase errors. As is apparent from (12), κ_u depends on N, M and the ratio between them $\omega = \frac{N}{M}$.

The indicated relationships are illustrated by the graphs in figs. 5 and 6 with $\alpha = 0$. It is apparent from fig. 5 that in the antenna with constant number of sections ($N=\text{const}$), the greatest gain in σ_{uM}^2 is obtained with sampling the phase errors at the end of each section (with $N=12, M=1, \kappa_u \sim 70$).

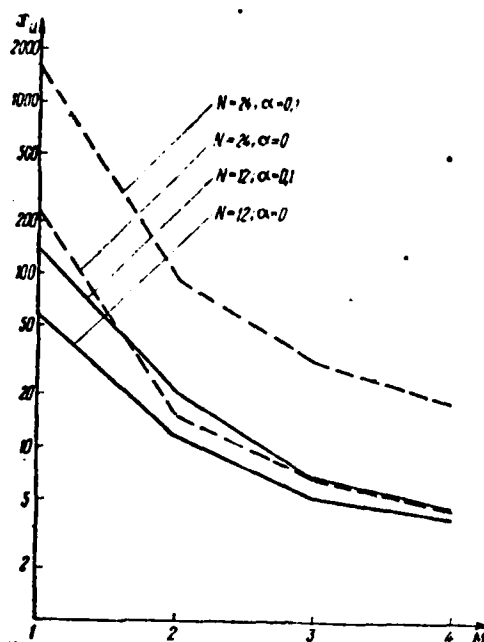


Figure 5.

With an increase in the number of sections M in the group, the quantity χ_u is diminished and the rate of its decrease slows down. A more significant "gain" in directional dispersion of the main BP maximum is obtained in the antennas with greater N (fig. 6, curves $M = \text{const}$). However, with an increase in M (reduction in ω), the dependence of χ_u on N becomes weaker and the gain practically becomes the same for any N with $\omega=2$ (fig. 6). It is also apparent from this figure, that the quantity χ_u mainly depends on the number of groups and its evaluation can be made according to the formula $\chi_u \approx \frac{\omega^2}{3}$.

In analyzing the decrease in dg , by analogy with χ_u , we introduce into the examination a quantity χ_Δ which equals the ratio of decrease in dg in the absence of sampling of phase errors to the decrease in dg in the STWA with sampling of errors through M sections $\chi_\Delta = \frac{\Delta_N}{\Delta_M}$ [see formula (10)]. This quantity characterizes the "gain" in reducing the dg through the sampling. The dependence of χ_Δ on the parameters of sectioning is illustrated by a series of graphs presented in figs. 7 and 8. The numbers on the arrow in fig. 7 show the quantity χ_Δ with

M=1. Graphs with $\alpha = 0$ correspond to the examined case.

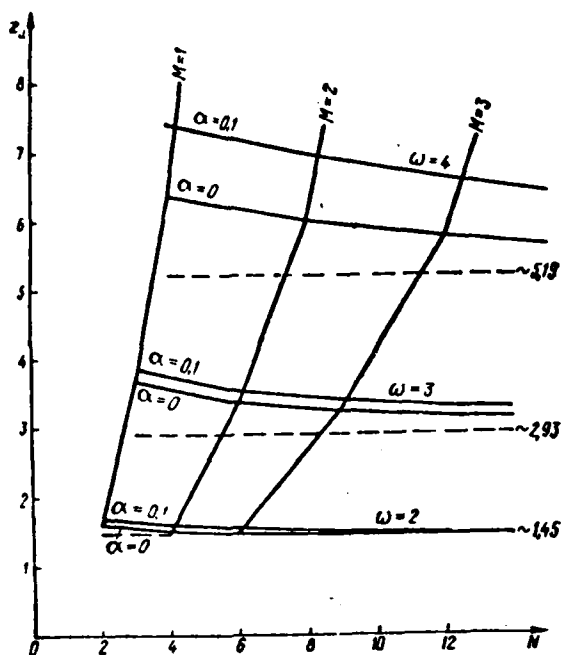


Figure 6.

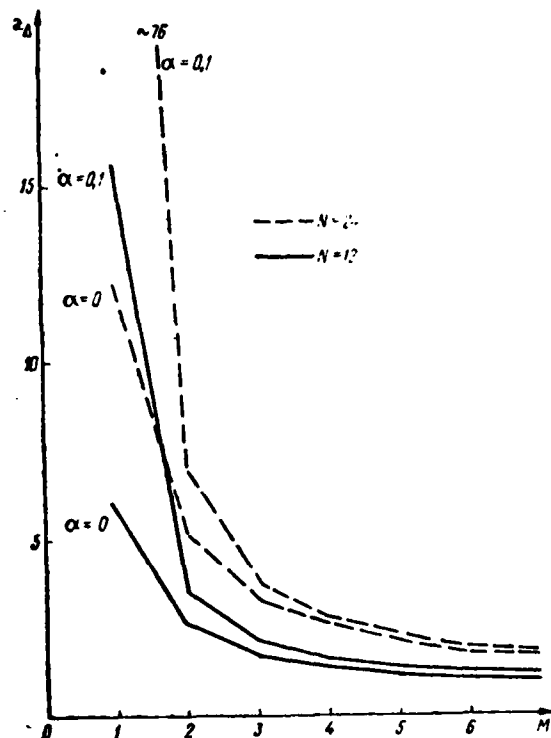


Figure 7.

It is apparent from the graphs that the nature of dependence of κ on M , N and ω is mainly the same as for κ_u . The difference is that with $N \gg 1$, the gain in dg because of error sampling can be estimated by the formula $\kappa_s \approx 0.3\omega + 0.4$ (in contrast to $\kappa_u \approx \frac{\omega^2}{3}$).

3. Sampling is made of the phase error through M sections in the presence of fluctuations in the wave number and errors in the sites of junction ($\sigma_y^2 \neq 0$, $M \neq N$).

In this case, the decrease in dg and dispersion of the course of the main maximum is described by expressions (10) and (12) respectively.

As follows from these expressions, with $M = \text{const}$ and with unchanged length of the sections 1, with an increase in the number of sections N

(and this means an increase in the length of the antenna), the decrease in dg remains practically unchanged, and the directional dispersion of the main maximum diminishes.

Thus, when sampling of the phase errors is used, there are no limitations which are usually placed on the length of the antenna because of the presence of errors in the APD.

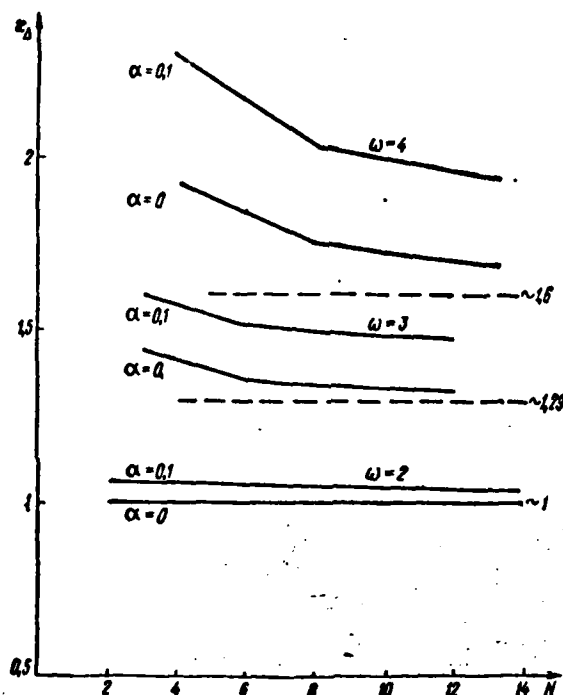


Figure 8.

The dependences of the quantities x_u and x_Δ on the sectioning parameters and the size of the errors at the sites of junction α are presented in figures 5-8.

As is apparent from the figures, the appearance of the dependences of gain in the reduction in dg and dispersion of direction of the main maximum with $\alpha \neq 0$ on the quantities ω , N , M are preserved the same as in the case of $\alpha = 0$. The most significant discrepancies in the numerical values x_u and x_Δ are observed with small M . This is associated with the fact that with small M , the effect of $\Delta\gamma_1$ on the antenna parameters

are practically excluded.

We note that in evaluating the effect of the sectioning methods and rejection of sections on the decrease in dg and the amount of directional dispersion of the main BP maximum, it is necessary to use the ratios (10)-(12) and the graphs in fig. 2. It is evident that during selective arrangement of the sections, the quantity σ_{uM}^2 is smaller than during random arrangement. The increase in the percentage of rejection of the sections also results in a decrease in σ_{uM}^2 . Similar results can be drawn in relation to the quantity Δ_M .

In conclusion, the authors express their gratitude to Professor Ya. S. Shifrin for attention to this work.

Appendix

In order to obtain a formula for the course of the direction of the main BP maximum, we initially present a technique to solve equations of the type:

$$A_u F(u, b) = 0, \quad (A.1)$$

where

$F(u, b)$ --beam pattern of antenna in presence of errors in APD,

A_u --certain linear (in relation to u) operator,

b --certain statistical small parameter of errors in APD.

In this case, one can view (A.1) as an equation which implicitly assigns u as the function of b , and presents u in the form of a Maclaurin series, limited only by the first m terms:

$$u(b) \approx \sum_{\kappa=0}^m \frac{u_b^{(\kappa)}(0)}{\kappa!} b^\kappa. \quad (A.2)$$

The derivatives of $u_b^k(0)$ which are included in (A.2) are defined from the known rules for differentiating implicit functions [4].

Thus, for example,

$$u'_b(0) = - \frac{A_u F'_b(u, b)}{A_u F'_u(u, b)} \bigg|_{b=0};$$

$$u''_{bb} = - \frac{A_u \{ F''_{bb}(u_0, 0) + 2F''_{ub}(u_0, 0) u'_b(0) + F''_{uu}(u_0, 0) [u'_b(0)]^2 \}}{A_u F'_u(u_0, 0)}.$$

The quantity u_0 is a solution to equation $A_u F(u, 0) = 0$, where $F(u, 0)$ is the beam pattern of the antenna in the absence of errors, and is usually considered to be known.

With fairly small values in the expansion of (A.2), we can limit ourselves to the first two terms. Then

$$\Delta u = u(b) - u_0 - b \frac{A_u F'_b(u_0, 0)}{A_u F'_u(u_0, 0)}. \quad (\text{A.3})$$

With definite u , from formula (A.3) one can find the quantity of expansion of the BP position of zeros or equisignal direction in the BP, etc. In particular, with $A_u = \frac{\partial}{\partial u}$, formula (A.3) determines the directional course of the main BP maximum.

Bibliography

1. Shifrin, Ya. S.; and Korniyenko, L. G. "Statistics of the Field of Linear Sectional Antenna," Khar'kov, Edition XGY, Interdepart. Sci. Tech. Assoc., Radiotekhnika, No. 6, 1968, pp 11-19.
2. Zamyatin, V. I.; and Korniyenko, L. G. "Statistics of the Field of Traveling Wave Sectional Antenna," Radiotekhnika i elektronika, Vol. 15, No. 6, 1970, pp 1297-1300.
3. Zhoglev, Ye. A.; and Antropov, N. M. "Certain Methods of Attenuating the Effect of Phase Errors on Beam Patterns of Antennas Consisting of Linear Emitters with Traveling Wave," Antenny [Antennas], ed. by A. A. Pistol'kors, Moscow, Svyaz', No. 9, 1970.
4. Smirnov, V. S. Kurs vysshey matematiki ["Course in Higher Mathematics"], Moscow, Nauka, Vol. 1, 1967.

STATISTICS OF THE FIELD OF FOCUSED SYSTEMS

A. S. Yevseyev

Summary

The average characteristics of a focal spot are examined in the focusing area when there are random phase errors. The calculated correlations and graphs make it possible to estimate the decrease in field intensity in the focus and the expansion of the focal spot depending on the numerical characteristics of the phase errors.

Introduction

By focused antennas we usually mean those antennas in which the quadratic component for the difference in the course of beams from the antenna to the observation point located in Fresnel's zone is compensated for in some manner.

It is common knowledge that in Fresnel's zone, the expression for the difference in the course of the beams (fig. 1)

$$\kappa(R-R_1) \approx \kappa z \sin \theta - \frac{\kappa z^2 \cos^2 \theta}{2R} + \frac{\kappa z^2 \sin \theta}{2R^2} + \dots \quad (1)$$

does not take into consideration the terms of the series above the second degree in relation to z . By artificially introducing phase distribution of the field along the antenna equal to $\frac{\kappa z^2 \cos^2 \theta_0}{2R_0}$, we can, in the limits of small angles in the region $\theta \approx \theta_0$ at distance R_0 (focal distance), obtain the same field as in the distant zone of the antenna. With $R \neq R_0$, the distribution of the field is different than in the distant zone.

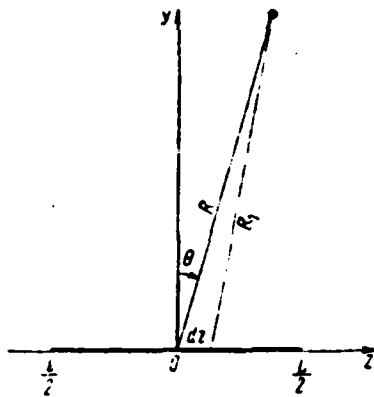


Figure 1.

Interest in the focused systems has recently noticeably increased since they can be used to solve a number of important problems. Thus, for example, the use of focusing permits measurement of the beam pattern of large antennas at reduced distances, expansion of the potentialities of the antennas of side-scanning radar stations, etc.

In this respect, it is definitely important to study the parameters of the focused systems when there are inevitably existing

different destabilizing factors. This work examines the average intensity and width of the focal spot of a focused antenna when there are phase errors along the antenna. Phase errors can be dictated both by inaccurate fabrication and instabilities in the parameters of the elements of the antenna itself (internal errors), and by the presence of fluctuations in the refraction index of the medium (external errors).

Original Correlations

The field intensity of the focused linear antenna in Fresnel's zone with accuracy to a constant multiplier equals [1]:

$$P_0(\psi, a) = \int_{-1}^{+1} A(x) A(x_1) e^{i\psi(\lambda - x_1) + i\pi(x_1^2 - x^2)} dx dx_1, \quad (2)$$

where $A(x)$ -- amplitude distribution, $x = \frac{2z}{L}$ -- relative coordinate, $\psi = \frac{\pi L}{\lambda} (\sin \theta - \sin \theta_0)$ -- generalized angle, θ_0 -- direction of the radiation maximum, $a = \frac{\pi L^2}{8} \left(\frac{\cos^2 \theta}{R} - \frac{\cos^2 \theta_0}{R_0} \right)$ -- focusing parameter.

In the case of uniform amplitude distribution $A(x) = A_0 = \frac{1}{2}$, the expression for $P_0(\psi, a)$ looks like

$$P_0(\psi, a) = \frac{\pi}{2a} \{ [C(\tau) + C(\xi)]^2 + [S(\tau) + S(\xi)]^2 \}, \quad (3)$$

where $\tau = a \left(1 - \frac{\psi}{2a} \right)^2$, $\xi = a \left(1 + \frac{\psi}{2a} \right)^2$, $C(\tau)$, $S(\tau)$ -- Fresnel's integrals.

With $R = R_0$ and $\theta \approx \theta_0$, one can consider that $a = 0$. Then $P_0(\psi, 0) = \frac{\sin^2 \psi}{\psi^2}$.

The transverse dimensions of the focal spot (at the level of half power) correspond to the width of the antenna BP in Fraunhofer's zone, and are determined by the known correlation: $2\Delta\psi_{0.5P} = 2.78$. With $\psi = 0$, we have $\tau = \xi = a$, and

$$P_0(\psi, a) = P_0(0, a) = \frac{2\pi}{a} [C^2(a) + S^2(a)].$$

The graph for the dependence of $P_0(0, a)$ on the focusing parameter is presented in fig. 2 (solid curve). By assuming $P_0(0, a) = 0.5$, we find the longitudinal dimensions of the focal spot $2\Delta a_{0.5P} \approx 4.7$.

The ratio of the longitudinal spot dimension to its width in relative units $\frac{2\Delta a_{0.5P}}{2\Delta\psi_{0.5P}} \approx 1.68$.

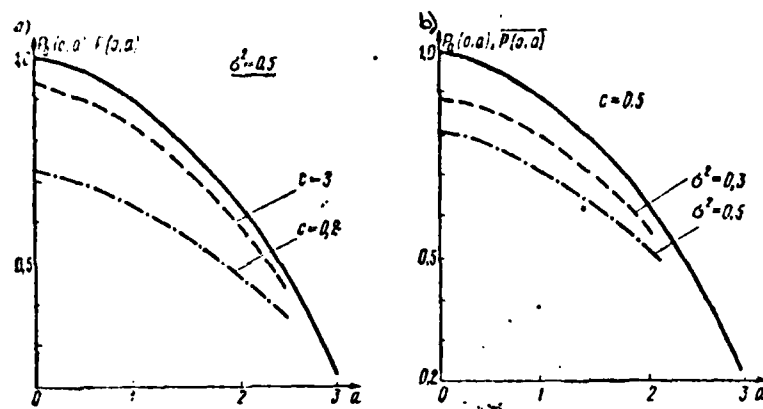


Figure 2.

Average Field Intensity

When there are random phase errors $\phi(x)$ along the antenna, the individual realization of the field intensity will be

$$P(\psi, a) = \frac{1}{4} \int_{-1}^{+1} \int_{-1}^{+1} e^{i[\phi(x) - \phi(x_1)]} e^{i\phi(x-x_1) + ia(x_1^2 - x^2)} dx dx_1. \quad (4)$$

The statistics $P(\psi, a)$ depends on the numerical characteristics of the phase errors $\phi(x)$. We will examine two types of errors: internal and external.

The following assumptions are usually correct for the first type of errors: the errors are small and stationary over the length of the antenna, i.e., the average value $\overline{\phi(x)} = 0$, the dispersion $\overline{\phi^2(x)} = \sigma^2 < 1$ and the correlation coefficient $r(x, x_1) = r(x - x_1)$. It evidently makes sense to study the effect of these errors on the field intensity for such focusing areas where the standard value of the phase considerably exceeds the quantity of the negligible third term in the series in expression (1), i.e., $\sigma \gg \frac{\kappa L^3 \sin \theta}{16R^2}$. At the same time [1] $R > 0.62 \sqrt{L^3/\lambda}$.

The latter inequality determines the near boundary of the Fresnel's zone. When the wave spreads in the turbulent medium, the errors (fluctuations) may have a random quantity. To describe the errors, the literature uses both Gaussian and Kolmogoroff models of an inhomogeneous medium. We will examine both models below.

1. We will first study the average field intensity when there are errors of internal origin. By averaging the correlation (4) for a group of realizations, or for time, we obtain

$$P(\psi, a) = P_0(\psi, a)(1 - \sigma^2) + \sigma^2 Y(\psi, a),$$

where

$$Y(\psi, a) = \frac{1}{4} \int_{-1}^{+1} \int_{-1}^{+1} r(x-x_1) e^{i\psi(x-x_1) + ia(x_1^2 - x^2)} dx dx_1. \quad (5)$$

We will further adopt the correlation coefficient of phase errors in the Gaussian form $r = \exp\left[-\frac{(x-x_1)^2}{c^2}\right]$, where $c = \frac{2\rho}{L}$ -- relative radius of the error correlation. The integral $Y(\psi, a)$ for this case is computed approximately in appendix 1 (the computation used the results of publication [3]).

Formula (5) and the results of appendix 1 make it possible to calculate the average field intensity with different values of the parameters a , ψ , c and σ^2 .

With $a \approx 0$, the expression for $\overline{P(\psi, 0)}$ coincides with the analogous expression for the average beam pattern in the distant zone that was studied in detail in publication [2]. It also presents curves which characterize the decrease in field intensity in the main direction, and curves which determine the width of the beam pattern. These curves make it possible to determine the decrease in field intensity in the focus (fig. 2.3) of work [2] and the transverse dimensions of the focal spot (fig. 2.15, work [2]).

With $\psi = 0$,

$$P(0, a) = P_0(0, a)(1 - \sigma^2) + \sigma^2 Y(0, a), \quad (6)$$

where

$$Y(0, a) = \frac{1}{4} \int_{-1}^{+1} \int_{-1}^{+1} e^{-\frac{(x-x_1)^2}{c^2} + ia(x_1^2 - x^2)} dx dx_1.$$

Figure 2a,b shows the dependence of $\overline{P(0, a)}$ on a for a series of values of σ^2 and c . The curves of fig. 3 define the width of the focal spot in a longitudinal direction.

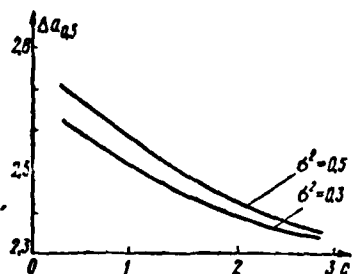


Figure 3.

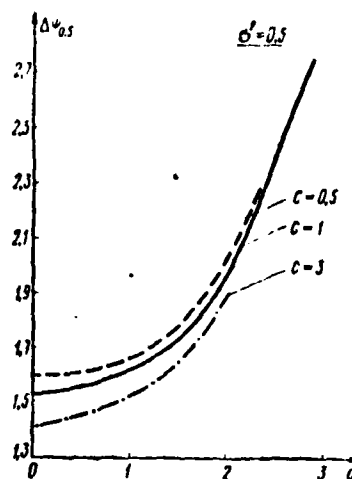


Figure 4.

By analyzing figs. 2,3 and 4 we can draw the following conclusions.

a) The presence of phase errors results in a decrease in field intensity in the focus and expansion of the focal spot, and the transverse and longitudinal dimensions of the spot increase roughly equally (thus, for example, with $c=0.5$ and $\sigma^2=0.5$ $\frac{2\Delta a_{0.5P}}{2\Delta \psi_{0.5P}} = 1.65$);

b) Reduction in the relative radius of the correlation of phase errors or increase in their dispersion causes expansion of the focal spot and reduction in field intensity near the focusing point.

2. We will now examine the effect of turbulence of the medium on field intensity of the focused systems, after limiting ourselves to consideration of only phase fluctuations. If in order to describe the medium, we adopt the Gaussian model of an inhomogeneous medium, then in this case, the results of the calculations obtained in section 1 will be completely correct. In this case one should only bear in mind that the dispersion of phase errors is determined by the ratio [2] $\sigma_{\psi}^2 = \frac{1}{2} \frac{\pi}{\lambda} (\overline{\Delta n})^2 \kappa^2 l_0 R$, where $(\overline{\Delta n})^2$ -- dispersion of fluctuations in the refraction index of the medium, while the radius of the correlation c is roughly equal to the average scale of inhomogeneity l_0 .

The calculation looks somewhat different for the case where the Kolmogoroff model of turbulent medium is used.

In this case [4]

$$e^{i[\varphi(x) - \varphi(x_1)]} = \exp[-C_\varphi^2 |x - x_1|^{5/3}],$$

where $C_\varphi^2 = (550BSR\lambda^{-1/3}) \left(\frac{L}{\lambda}\right)^{5/3}$.

Here R--length of wave path in turbulent medium; B--parameter which characterizes the intensity of the dielectric inhomogeneities [$B \approx (10^{-18} - 10^{-16}) \text{ cm}^{-2/3}$], on the average $B = 1.3 \times 10^{-17} \text{ cm}^{-2/3}$

$$S = \begin{cases} 0.5 & \text{with } |z - z_1| \ll \sqrt{\lambda R}, \\ 1 & \text{with } |z - z_1| \geq \sqrt{\lambda R}. \end{cases}$$

The 5/3 law for the structural function of the phase is confirmed all the way to the bases $|z - z_1| = 4 \text{ km}$ [5].

As previously, in the absence of fluctuations in the phase, the field intensity is determined by the ratio (3).

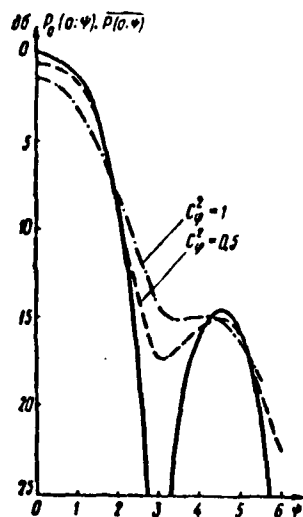


Figure 5.

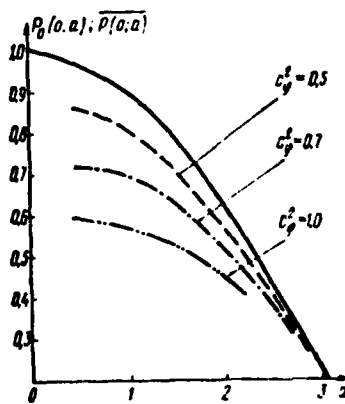


Figure 6.

The average field intensity

$$\overline{P(\varphi, a)} = \frac{1}{4} \int_{-1}^{+1} e^{-C_\varphi^2 |x - x_1|^{5/3} + i\varphi(x - x_1) + i\varphi(x_1^2 - x^2)} dx dx_1. \quad (7)$$

The integral in correlation (7) is computed approximately in appendix 2.

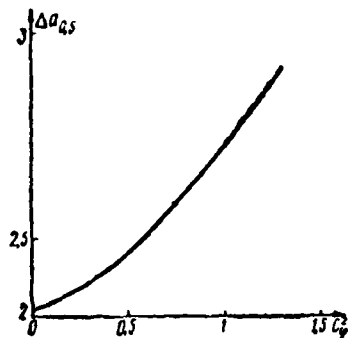


Figure 7.

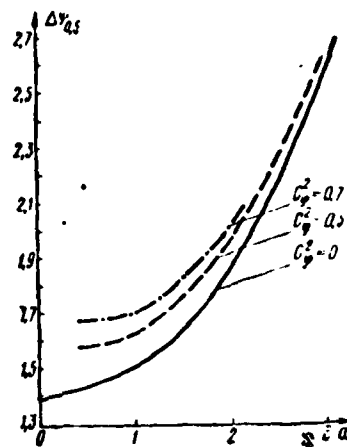


Figure 8.

By assuming $a=0$, we find from correlation (7)

$$\overline{P(\psi, 0)} = \frac{1}{4} \int_{-1}^{+1} \int_{-1}^{+1} e^{-C_{\phi}^2 |x-x_1|^{5/3} + i\psi(x-x_1)} dx dx_1. \quad (8)$$

The curves for average field intensity which are computed from this formula for the two values C_{ϕ}^2 are presented in fig. 5. The graph (fig. 6) characterizes the dependence of field intensity near the focusing point on the parameter a . Figure 7,8 presents the graphs which determine the effect of C_{ϕ}^2 on the longitudinal and transverse dimensions of the focal spot. These graphs can be used to estimate the linear dimensions of the spot at the assigned distance when the antenna is transmitting. From an analysis of the presented graphs we can draw the conclusion that with an increase in the phase errors, the field intensity drops, while the transverse and longitudinal dimensions of the focal spot increase equally.

When the graphs are used, it is necessary to bear in mind that the quantities C_{ϕ}^2 and a are mutually dependent, since both C_{ϕ}^2 and a are determined by the quantities R , L and λ . The distance R_0 and the parameter of turbulence B are independent parameters.

In conclusion, the author expresses deep gratitude to Ya. S. Shifrin for supervising this work, and L. G. Korniyenko for advice and attention to it.

Appendix 1.

1. We cannot precisely compute the integral

$$Y = \int_{-1}^{+1} \int_{-1}^{+1} e^{-\frac{(x-x_1)^2}{c^2} + i\psi(x-x_1) + i\psi(x_1^2-x^2)} dx dx_1$$

with random c and a . Therefore we will examine the asymptotic expressions for Y with $c \ll 1$ and $c \gg 1$:

a) with $c \ll 1$

By using the variables $u = \frac{x_1 - x}{\sqrt{2}}$ and $v = \frac{x + x_1}{\sqrt{2}}$, we have

$$Y = \int_0^{\sqrt{2}} e^{-\frac{2u^2}{c^2} - i\sqrt{2}\psi u} dv \int_{-(\sqrt{2}-u)}^{\sqrt{2}-u} e^{i2auv} du + \int_{-\sqrt{2}}^0 e^{-\frac{2u^2}{c^2} - i\sqrt{2}\psi u} \times \\ \times \int_{-(\sqrt{2}+u)}^{\sqrt{2}+u} e^{i2auv} dv = 2 \int_0^{\sqrt{2}} e^{-\frac{2u^2}{c^2} - i\sqrt{2}\psi u} \sin \frac{2au(\sqrt{2}-u)}{au} du. \quad (A.1)$$

Passing further to a new variable $y = \frac{\sqrt{2}u}{c}$, we obtain

$$Y = 2 \int_0^{\infty} e^{-y^2 - i\psi c y} \frac{\sin 2acy \left(1 - \frac{cy}{2}\right)}{ay} dy - \\ - 2 \int_{2/c}^{\infty} e^{-y^2 - i\psi c y} \frac{\sin 2acy \left(1 - \frac{cy}{2}\right)}{ay} dy. \quad (A.2)$$

With accuracy to the quantity $\frac{c^4}{8} e^{-4/c^2}$ we have

$$Y \approx \frac{\pi}{4a} \left[\Phi\left(\frac{\eta_1}{2\sqrt{\rho_1}}\right) + \Phi\left(\frac{\eta_1}{2\sqrt{\rho_2}}\right) + \Phi\left(\frac{\eta_2}{2\sqrt{\rho_1}}\right) + \Phi\left(\frac{\eta_2}{2\sqrt{\rho_2}}\right) \right] + \\ + \frac{1}{ia} \left[\int_0^{\frac{\eta_1}{2\sqrt{\rho_1}}} F(\eta) d\eta - \int_0^{\frac{\eta_2}{2\sqrt{\rho_2}}} F(\eta) d\eta + \int_0^{\frac{\eta_2}{2\sqrt{\rho_1}}} F(\eta) d\eta - \int_0^{\frac{\eta_1}{2\sqrt{\rho_2}}} F(\eta) d\eta \right] - \\ - \frac{1}{a} \operatorname{arctg} \beta, \quad (A.3)$$

where $\eta_{1,2} = 2ac \pm c\psi$, $\beta = ac^2$, $\rho_{1,2} = 1 \pm i\beta$, $\Phi(\rho) = \frac{2}{\sqrt{\pi}} \int_0^{\rho} e^{-t^2} dt$ -- integral of probability.

By designating $\frac{\eta_1}{2\sqrt{\rho_1}} = z_{01} = a_1 + ib_1$, $\frac{\eta_2}{2\sqrt{\rho_2}} = z_{02} = a_2 + ib_2$ and by taking into account $\rho_1 = \rho_2^*$, $\Phi(z^*) = \Phi^*(z)$, with the help of the known expression for

$$F(z) = \sum_{n=0}^{\infty} \frac{(-1)^n 2^n \operatorname{Im} z_0^{2n+1}}{1 \cdot 3 \cdot \dots \cdot (2n+1)(2n+2)}$$

we will write the integral in the following form:

$$\begin{aligned} \operatorname{Re} Y = \frac{1}{2a} & \left\{ \pi [\operatorname{Re} \Phi(z_{01}) + \operatorname{Re} \Phi(z_{02})] + 4 \sum_{n=0}^{\infty} \times \right. \\ & \frac{(-1)^n 2^n \operatorname{Im} z_{01}^{2n+1}}{1 \cdot 3 \cdot \dots \cdot (2n+1)(2n+2)} + 4 \sum_{n=0}^{\infty} \frac{(-1)^n 2^n \operatorname{Im} z_{02}^{2n+1}}{1 \cdot 3 \cdot \dots \cdot (2n+1)(2n+2)} \\ & \left. - 2 \operatorname{arctg} \beta \right\}. \end{aligned} \quad (\text{A.4})$$

Expression (A.3) has a broad area of application, practically to $c \approx 1$.

With $c \leq 0.5$, by assuming $\beta \leq 1$, we have

$$\operatorname{Re} Y \approx \frac{1}{2a} \left\{ \pi \left[\Phi\left(\frac{\eta_1}{2}\right) + \Phi\left(\frac{\eta_2}{2}\right) \right] + \eta_1 \beta F\left(\frac{\eta_1}{2}\right) + \eta_2 \beta F\left(\frac{\eta_2}{2}\right) - 2\beta \right\}. \quad (\text{A.5})$$

b) $c \gg 1$.

By using the expansion of the exponential function $e^{-x^2} \approx 1 - x^2$, we will write the correlation (A.1) with accuracy to terms of the second order of smallness in the form:

$$\operatorname{Re} Y = 4P_0(\psi, a) - \frac{4}{ac^2} \int_0^{\sqrt{2}} u \cos \sqrt{2} \psi u \sin 2au (\sqrt{2} - u) du. \quad (\text{A.6})$$

Here $P_0(\psi, a) = F_0(\psi, a) F_0^*(\psi, a)$,

$$\begin{aligned} F_0(\psi, a) &= \frac{1}{2} \int_{-1}^{+1} e^{i\psi x - iax^2} dx = e^{i\frac{\psi^2}{4a}} \sqrt{\frac{\pi}{2a}} \left\{ C \left[a \left(1 - \frac{\psi}{2a} \right)^2 \right] + \right. \\ & \left. + C \left[a \left(1 + \frac{\psi}{2a} \right)^2 \right] - i S \left[a \left(1 - \frac{\psi}{2a} \right)^2 \right] - i S \left[a \left(1 + \frac{\psi}{2a} \right)^2 \right] \right\}. \\ P_0(\psi, a) &= \frac{\pi}{2a} \{ [C(\tau) + C(\xi)]^2 + [S(\tau) + S(\xi)]^2 \}. \end{aligned}$$

The integral in expression (A.6) is computed in appendix 2.

Appendix 2

We will examine the integral

$$Y = \frac{1}{4} \int_{-1}^{+1} \int_{-1}^{+1} e^{-C_\phi^2 |x-x_1|^{5/3} + 14(x-x_1) + 16(x_1^2-x^2)} dx dx_1. \quad (A.2.1)$$

By replacing the variables $u = \frac{x_1-x}{2}$, $v = \frac{x+x_1}{2}$, we transform (1) into the form:

$$\begin{aligned} Y &= \frac{1}{2} \int_{-1}^{+1} e^{-3.18 C_\phi^2 |u|^{5/3} - 124u} du \int_{-(1-|u|)}^{1-|u|} e^{14av} dv = \\ &= \frac{1}{2} \int_0^1 e^{-3.18 C_\phi^2 u^{5/3} - 124u} \frac{\sin 4au(1-u)}{au} du. \end{aligned} \quad (A.2.2)$$

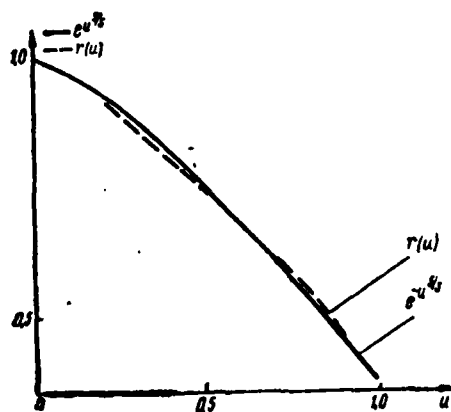


Figure 9.

It is not possible to compute (A.2.2) in the quadratures. For an approximate computation, we will use the method of approximating functions. The most suitable is the function $r(u) = \cos 1.2u - 0.08 \sin \pi u$ (fig. 9.). We will write the quantity $3.18 C_\phi^2 = n + \alpha$, where n -- the nearest whole number. Then $|\alpha| \leq 0.5$ and $r^\alpha \approx 1 - 0.72\alpha u^2 - \alpha 0.08 \sin \pi u$. It is easy to see that in the expression for $r^{n+\alpha}$ there are trigonometric functions of degrees $1, 2, \dots, h$. By using the expansion of these functions through the function of multiple arcs, one can reduce the expression (A.2.2) to the sum of integrals of the type:

$$I_{1,2} = \int_0^1 u \sin 4au (1-u) \frac{\cos \gamma u}{\sin \gamma u} du; \quad I_{3,4} = \\ = \int_0^1 \frac{\sin 4au (1-u)}{au} \frac{\cos \gamma u}{\sin \gamma u} du$$

After the computations, we have

$$I_1 = \frac{1}{2} \left\{ \frac{1}{8a} \cos(4aB_1^2 - ab_1^2) - \frac{1}{4a} + \frac{b_1}{4} \right\} \frac{\pi}{2a} [S(ab_1^2) - S(4aB_1^2)] \cos ab_1^2 + \\ + \frac{b_1}{4} \sqrt{\frac{\pi}{2a}} \sin ab_1^2 [C(ab_1^2) - C(4aB_1^2)] + \frac{1}{8a} \cos(4aB_1^2 - ab_1^2) - \\ - \frac{b_1}{4} \sqrt{\frac{\pi}{2a}} \cos ab_1^2 [S(ab_1^2) + S(4aB_1^2)] + \frac{b_1}{4} \frac{\pi}{2a} \sin ab_1^2 [C(ab_1^2) - \\ + C(4aB_1^2)] \Big\}, \\ I_2 = \frac{1}{2} \left\{ \frac{1}{8a} \sin(4aB_1^2 - ab_1^2) - \frac{b_1}{2} \sqrt{\frac{\pi}{2a}} \cos ab_1^2 [C(4aB_1^2) - C(ab_1^2)] - \right. \\ \left. - \frac{b_1}{4} \sqrt{\frac{\pi}{2a}} \sin ab_1^2 [S(4aB_1^2) - S(ab_1^2)] - \frac{1}{8a} \sin(4aB_1^2 - ab_1^2) - \right. \\ \left. - \frac{b_1}{4} \right\} \sqrt{\frac{\pi}{2a}} \cos ab_1^2 [C(4aB_1^2) + C(ab_1^2)] - \frac{b_1}{4} \sqrt{\frac{\pi}{2a}} \sin ab_1^2 \times \\ \times [S(4aB_1^2) + S(ab_1^2)] \Big\},$$

where $b_1 = \frac{\gamma}{4a} - 1$, $b_2 = \frac{\gamma}{4a} + 1$, $B_1 = 1 + \frac{b_1}{2}$, $B_2 = 1 - \frac{b_2}{2}$,

$$I_3 = P_0\left(\frac{\gamma}{2}, a\right) + P_0\left(-\frac{\gamma}{2}, a\right), \quad I_4 = P_0\left(\frac{\gamma}{2}, a\right) - P_0\left(-\frac{\gamma}{2}, a\right).$$

Bibliography

1. Skaniroyushchiye antennoye sistemy SVCh ["Scanning Antennas of the SHF System"], Trans. from English, Moscow, Sovetskoye radio, 1966.
2. Shifrin, Ya. S. Voprosy statisticheskoy teorii antenn ["Questions of the Statistical Theory of Antennas"], Moscow, Sovetskoye radio, 1970.
3. Landkof, N. S.; and Shifrin, Ya. S. "Question of the Effect of Fluctuations on the Diffraction Image of a Focusing System," Trudy ARTA, No. 46, 1960.
4. Tatarskiy, V. I. Teoriya fluktuatsionnykh yavleniy v turbulentnoy atmosfere [Theory of Fluctuation Phenomena in a Turbulent Atmosphere], Moscow, Nauka, 1967.
5. Tatarskiy, V. I. "Radio Physical Methods of Studying the Atmosphere," Izvestiya vuzov. Ser. Radiofizika, No. 4, 1960, pp. 551-558.

EFFICIENCY AND INPUT IMPEDANCE OF PLANAR
EMITTER PLACED NEAR THE INTERFACE

V. P. Kul'tsep

Summary

Strict general formulas are derived for complex input impedance of a random plane-parallel interface of an emitter with assigned current distribution. A calculation is made of the dependence of the input impedance and efficiency of the inphase planar disk emitter on its radius and the distance from the interface for emitters of any size.

Introduction

When an emitter is placed near the interface of two media 1 and 2 with different permeabilities ϵ_1 and ϵ_2 , the emitted energy is generally redistributed towards the medium with greater permeability. If the radiation towards medium 1 is useful, then the efficiency of the emitter is defined as the ratio of the active power emitted into medium 1 to the complete active power fed to the emitter.

It is important to determine the maximum efficiency that can be obtained from a planar emitter of assigned finite parameters which is placed parallel to the interface.

Initial Correlations

We will use the Hansen-Bekerly method to compute the efficiency. It has been used repeatedly to determine the efficiency of emitters located near the interface in the same medium 1 to which it is desirable to direct the radiation maximum [1,2].

We will examine another case here where the emitter is located in medium 2, while it is desirable to direct the radiation to medium 1.

Assume that the emitter is assigned in the form of distribution of the current density vector i in a certain volume V . One can show (see the appendix) that the complex power which is transferred through the plane $z=z_1$ is located below the interface, but above the emitter (fig. 1),

$$P_1(z) = 60\pi^2 \kappa \sum_{n=-\infty}^{\infty} \left[\int_0^{\infty} (1 - \alpha_n e^{-i2m_n z}) (1 + \alpha_n e^{-i2m_n z})^* e^{-2zJnm_n} |f_{2n}^-|^2 \frac{f_{2n}^2 dl}{m_2} + \frac{\kappa_2}{\kappa_1} \int_0^{\infty} (1 - \alpha_n e^{-i2m_n z})^* (1 + \alpha_n e^{-i2m_n z}) e^{-2zJnm_n} |f_{3n}^-|^2 \frac{f_{3n}^2 dl}{m_2} \right] \quad (1)$$

The complex power which is transferred through the plane $z=z_1$ located below the emitter:

$$P_1(z) = 60\pi^2 \kappa \sum_{n=-\infty}^{\infty} \left[\int_0^{\infty} (f_{2n}^- + \alpha_n f_{2n}^+) (f_{2n}^- + \alpha_n f_{2n}^+)^* e^{2zJnm_n} \frac{f_{2n}^2 dl}{m_2} + \frac{\kappa_2}{\kappa_1} \int_0^{\infty} (f_{3n}^- + \alpha_n f_{3n}^+) (f_{3n}^- + \alpha_n f_{3n}^+)^* e^{2zJnm_n} \frac{f_{3n}^2 dl}{m_2} \right] \quad (2)$$

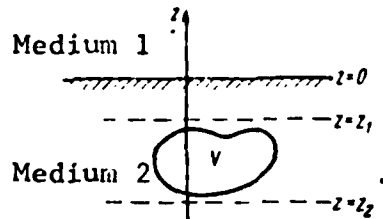


Figure 1.

In these expressions:

$$\kappa_i = \kappa \sqrt{\epsilon_i \mu_i}, \quad \kappa = 2\pi/\lambda, \quad \lambda - \text{wavelength}$$

$$m_i = \sqrt{\kappa_i^2 - \beta^2}, \quad \bar{\epsilon}_i = \epsilon_i + i60\sigma_i\lambda, \quad (3)$$

$$a_1 = \frac{\mu_1 m_2 - \mu_2 m_1}{\mu_1 m_1 + \mu_2 m_2}, \quad a_2 = \frac{\bar{\epsilon}_1 m_2 - \bar{\epsilon}_2 m_1}{\bar{\epsilon}_1 m_1 + \bar{\epsilon}_2 m_2},$$

$\mu_i, \epsilon_i, \sigma_i$ -- magnetic, dielectric permeabilities and conductance of media 1 and 2.

$$f_{in}^{\pm} = \frac{1}{2\pi l^2} \int_V i A_{zn}^{\pm} dV. \quad (4)$$

--coefficients of expansion of the vector potential according to the system of orthogonal vector functions whose projections onto the axes of the cylindrical coordinate system

$$\begin{aligned} A_{2nr}^{\pm} &= \frac{in}{r} J_n(lr) A^{\pm}, \quad A_{3nr}^{\pm} = \pm \frac{im_2}{\kappa_2} \frac{d}{dr} J_n(lr) A^{\pm}, \\ A_{2nq}^{\pm} &= -\frac{d}{dr} J_n(lr) A^{\pm}, \quad A_{3nq}^{\pm} = \mp \frac{m_2}{\kappa_2} \frac{n}{r} J_n(lr) A^{\pm}, \\ A_{2nz}^{\pm} &= 0, \quad A_{3nz}^{\pm} = \frac{\beta}{\kappa_2} J_n(lr) A^{\pm}, \end{aligned} \quad (5)$$

where $A^{\pm} = e^{i(n\varphi \pm m_2 z)}$, r, φ, z -- coordinates of the points of volume V in which the distribution of the current density vector i is assigned, J_n -- Besselian function; the asterisk designates the complex-conjugated quantity.

Expressions (1) and (2) generally do not make it possible to find the complete power fed to the emitter which is located in the medium with losses, since they do not take into consideration the power

which is stored and can be scattered in the volume between planes $z=z_1$ and $z=z_2$. If however, we examine a particular case of a planar emitter with zero extension on the z -axis, and we assume that $z_1=z_2=-h$, then expressions (1) and (2) make it possible to find quite accurate values for the assigned distribution of currents: $P_1(-h)$ --complete power emitted to the upper half-space; $P_2(-h)$ --complete power emitted to the lower half-space and $P_{\Sigma} = P_1(-h) + P_2(-h)$ --complete power fed to the emitter.

After dividing the complete power fed to the emitter into the square of the effective current value at the emitter inlet I_0^2 , we find the complete input impedance of the emitter

$$Z_{\Sigma} = R_{\Sigma} + iX_{\Sigma} = P_{\Sigma}/I_0^2. \quad (6)$$

If we substitute the coordinate of the interface $z=0$ into (1), then we obtain the power $P_1(0)$ which passes through the interface into medium 1, and the corresponding impedance

$$Z_{\Sigma} = R_{\Sigma} + iX_{\Sigma} = P_1(0)/I_0^2. \quad (7)$$

By definition given above, the efficiency

$$\eta = \frac{R_{\Sigma}}{R_{\Sigma}}. \quad (8)$$

We will introduce the designations

$$c_{2n} = \frac{1}{I_0} e^{\pm i m_n h} f_{2n}^{\pm}, \quad c_{3n} = \pm \frac{1}{I_0} \frac{\kappa_1}{m_n} e^{\pm i m_n h} f_{3n}^{\pm}. \quad (9)$$

Since in our case, $i_2=0$, then

$$c_{2n} = \frac{1}{2\pi I_0} \iint_S [(i_{\varphi} - i_r) \frac{n}{r} J_n(lr) - i_{\varphi} l J_{n-1}(lr)] e^{-in\varphi} r dr d\varphi, \\ c_{3n} = \frac{1}{2\pi I_0} \iint_S [(i_{\varphi} - i_r) \frac{n}{r} J_n(lr) + i_r \times l J_{n-1}(lr)] e^{-in\varphi} r dr d\varphi. \quad (10)$$

where i_z , i_{φ} , i_r --projections of vector i onto coordinate axes, S --area occupied by the assigned current distribution.

In addition, we designate:

$$u_1 = \frac{\kappa^2}{l^2} \sum_{n=-\infty}^{\infty} |c_{2n}|^2, \quad u_3 = \frac{\kappa^4}{l^2} \sum_{n=-\infty}^{\infty} |c_{3n}|^2. \quad (11)$$

Then expressions (6) and (7) for impedance of radiation and the input impedance can be written in a form convenient for calculations:

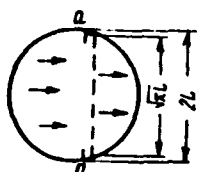
$$Z_1 = \frac{60\pi^2}{\kappa} \int_0^\infty \left[\frac{m_2}{m_1^2} (1 - |a_2|^2) u_2 + \frac{|m_2|^2}{\kappa_2^2} (1 - |a_3|^2) u_3 \right] e^{-2h\sqrt{m_1^2 - m_2^2}} \frac{ldl}{m_1}, \quad (12)$$

$$Z_{in} = \frac{120\pi^2}{\kappa} \int_0^\infty \left[\frac{m_2}{m_1^2} (1 + a_2 e^{12m_1 h}) u_2 + \frac{|m_2|^2}{\kappa_2^2} (1 - a_3 e^{12m_1 h})^* u_3 \right] \frac{ldl}{m_1}. \quad (13)$$

The cofactors of the integrands in (12) and (13) have a specific physical meaning. Thus, u_s --beam patterns of the emitter which have been averaged for the azimuth angle in a free space for perpendicularly (u_2) and parallel (u_3) polarized waves. The multipliers before u_s show how the beam pattern of the emitter changes because of the presence of an interface. The cofactor ldl/m_2 is the element of solid angle in medium 2 multiplied by k .

Input Impedance of Disk Emitter

Figure 2.



One can assume that among the planar inphase emitters of assigned area, the emitter of round shape with continuous and uniform distribution of the sources has an efficiency close to the highest.

We will examine the planar current disk of radius L (fig. 2) which is located in medium 2 parallel to the interface at depth h . It has a distribution of the current density vector which is constant in quantity and direction. Its projections look like:

$$I_r = I \cos \varphi, \quad I_\varphi = I \sin \varphi. \quad (14)$$

The direction of the current density vector is shown in fig. 2 by the arrows.

Current density I is linked to the input current I_0 by a coefficient which depends on the plan for connecting the source to the emitter. We will adopt this coefficient such that the current density on the disk equals the current density in a square emitter which is equidimensional in area. Then $I = I_0 / L\sqrt{\pi}$. This essentially means that the power source is connected to the disk by chord aa whose length equals the length of a side of the equidimensional square shown in fig. 2 by the dotted line.

By substituting conditions (14) into (10) in this case, and by integrating in the limits of the disk area, we find

$$c_{2n} = c_{3n} = \begin{cases} -\frac{i}{2\sqrt{\pi}} J_1(1L) & \text{for } n = \pm 1 \\ 0 & \text{for the remaining } n. \end{cases} \quad (15)$$

By substituting (15) into (11), and further into (13), we obtain an accurate expression for the input impedance of the disk with uniform distribution of the current density located near the interface of the medium with any parameters.

We will examine certain particular cases. Assume that the emitter is located on the interface ($h=0$) of two media without losses. Then with $1 < k_2$, the integrand in (13) will be real, while with $1 > k_2$ it is imaginary. By correspondingly dividing the integration interval in (13) into two parts, and with $1 < k_2$, making a replacement with the variable $l = k_2 \sin \vartheta$, we have

$$Z_{\text{in}} = \frac{60\pi}{V \epsilon_1} \left\{ \int_0^{\pi/2} J_1^2(\kappa_2 L \sin \vartheta) [(1 + \alpha_2) + \cos^2 \vartheta (1 - \alpha_2)] \frac{d\vartheta}{\sin \vartheta} - \right. \\ \left. - i \int_{\kappa_1}^{\infty} J_1^2(1L) \left[\frac{\kappa_2}{m_2} (1 + \alpha_2) + \frac{m_2}{\kappa_2} (1 - \alpha_2) \right] \frac{dl}{l} \right\}, \quad (16)$$

where ϑ is angle between the z -axis and the direction to the observation point.

It is apparent from here that the integrand in the first integral is the disk beam pattern. Thus, the disk example shows the known situation where the active part of the input impedance of the emitter is

determined by integrating its beam pattern in the region of real angles. It is new that for the selected power circuit, both the active and reactive part of the input impedance are strictly defined in Ohms.

We will find approximate expressions for the input impedance, by using the fact that a large part of the emitted power is concentrated in the region of the beam pattern maximum, i.e., near $\vartheta=0$.

If the dimensions of the emitter are great ($k_2L \gg 1$), then in the first term (16) one can assume that $m_2=k_2$, $m_1=k_1$, $\sin \vartheta = \vartheta$, and $\cos \vartheta = 1$, while the upper limit of integration is equal to infinity. Then

$$R_{ax} = \frac{120\pi}{\sqrt{\epsilon_1} + \sqrt{\epsilon_2}}. \quad (17)$$

If the emitter is located in a uniform medium ($\alpha_2=\alpha_3=0$), then its input impedance equals $60\pi/\sqrt{\epsilon_2}$ --half of the wave impedance of the medium. On the contrary, if the interface is completely reflecting ($\alpha_2=-\alpha_3=1$), then the input impedance of the emitter equals $120\pi/\sqrt{\epsilon_2}$.

As follows from (17), the active part of the input impedance of a large emitter located on the interface lies between these extreme values.

If, on the contrary, the radius of the emitter is very small, then the Besselian function in the first integral (16) can be replaced by the first term in the series, and by assuming $m_2=k_2$ and $m_1=k_1$, we find

$$R_{ax} = 40\pi (\kappa_2 L)^2 \frac{1}{\sqrt{\epsilon_1} + \sqrt{\epsilon_2}}. \quad (18)$$

Figure 3 shows the dependences of R_{ax} on the disk radius L which are obtained by numerical integration (16) with different values of ϵ_2 . It is apparent from the curves that if the radius of the disk is small, then the input impedance rises in proportion to the square of the radius of the disk in accordance with (18). With $k_2L=1.5$, the rise in impedance is slowed down, and with $k_2L=10$, the impedance practically reaches its limiting value, determined by (17).

The reactive part of the input impedance is determined by the second integral in (16). It is easy to see that with $L \rightarrow \infty$, the average value of the integrand diminishes as $1/L$. This does not guarantee

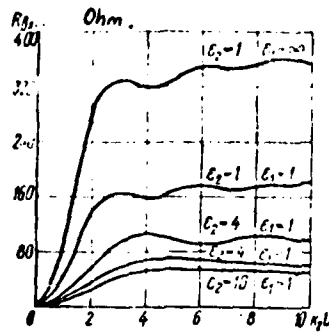


Figure 3.

convergence of the integral. This physically means that in order to maintain rectangular distribution of the current, it is necessary to create around the emitter an infinitely large reactive field, and consequently, the assigned distribution may not be realized with any value of L . If we examine the medium with losses, then with rectangular distribution of the current, the first integral in (16) differs. It determines the active part of the input impedance.

We will therefore examine current distribution which diminishes to zero on the edges of the emitter, for example:

$$i_x = \frac{I_0}{L\sqrt{\pi}} \cos \varphi \left[1 - \left(\frac{x}{L} \right)^2 \right], \quad i_y = \frac{I_0}{L\sqrt{\pi}} \sin \varphi \left[1 - \left(\frac{y}{L} \right)^2 \right]. \quad (19)$$

The current density in the center of the emitter is assigned here to be the same as in the emitter examined above with uniform distribution of the current density.

The expression for the input impedance with current distribution diminishing to the edge will be similar to (16). It yields the final result both for the active and for the reactive parts of the input impedance with any parameters of the medium 2.

As an example we will find one of the components of the active part of the input impedance associated with waves of parallel polarization. The real part of the second term in (13) corresponds to it. The precise expression for this component looks like:

$$R_a = \frac{60\pi\kappa}{l^2} \int_0^{\frac{l}{2}} J_0^2(H_l) \operatorname{Re} \left[\frac{m_2}{\kappa_2^2} (1 - a_2) \right] \frac{dl}{l^3}. \quad (20)$$

In this case, the convergence of the integral is guaranteed by the fact that the integrand with $l \rightarrow \infty$ diminishes as $1/l^2$.

We will approximately compute part of the integral in the limits from $1/L$ to ∞ . If the emitter is so small, that $|k_2 L| \ll 1$, then even on the lower limit of integration, one can assume that $m_2 = m_1 = 1$. In addition, we replace the square of the Besselian function by its average value for the period $1/\pi 1L$.

As a result, we have for the semiconducting medium

$$R_{11} = \frac{L}{4\pi\sigma_2} \quad (21)$$

Thus, the constant component of the emitter losses is obtained. The remaining components of the input impedance can also be obtained from the general expression (13) with the help of the approximations suggested in [2], or numerically.

Input Impedance of Square Emitter

We will now examine the case of a planar emitter of square shape (fig. 4). We will assume that its area is equal to the area of the round emitter with radius L examined above. Then the length of a side of the square emitter $2a = \sqrt{\pi}L$. We will assign uniform distribution of the current density of the type (14).

Determination of the coefficients c_{sn} with the help of (10) in the case of a square emitter runs into certain difficulties. We will therefore use the following concept for beam patterns of the emitter which have been averaged for the azimuth:

$$\begin{aligned} u_s &= \frac{\kappa^3}{8\pi^3 f_0^2} \int_{-\pi}^{\pi} \left| \int_{\xi} (i_x \cos \xi + i_y \sin \xi) e^{i l (x \sin \xi - y \cos \xi)} dx dy \right|^2 d\xi, \\ u_s &= \frac{\kappa^3}{8\pi^3 f_0^2} \int_{-\pi}^{\pi} \left| \int_{\xi} (i_x \sin \xi + i_y \cos \xi) e^{i l (x \sin \xi - y \cos \xi)} dx dy \right|^2 d\xi. \end{aligned} \quad (22)$$

where ξ —azimuth coordinate of the observation point, x, y ,—rectangular coordinates of the points on the emitter.

Expressions (22) can be obtained from (11) with the help of a generalized equation of closure, presenting the sum of the squares of the moduli c_{sn} in the form of an integral from the product of the sum

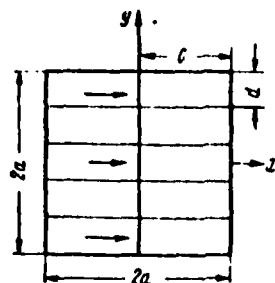


Figure 4.

times the sum complexly conjugate to it, and by further transforming the obtained expressions with the help of (10).

By assigning $i_x = I_0/2a$, $i_y = 0$ and by integrating in (22) for the area of a square with side $2a$, we find the beam pattern of the square emitter which is averaged for the azimuth.

$$u_2 = \frac{\kappa^2}{a^2 \pi^2 f^4} \int_{-\pi/2}^{\pi/2} \frac{\sin^2(al \sin \xi)}{\sin^2 \xi} \sin^2(al \cos \xi) d\xi. \quad (23)$$

If the dimensions of the emitter are large, then approximately

$$u_2 = \frac{\kappa^2 \sin^2 al}{2a\pi^2 f^4}. \quad (24)$$

The expression for u_3 is obtained analogously. Assume that the emitter is located on the boundary of two media without losses. Assuming, as with the derivation of (17), $m_2 = k_2$, $m_1 = k_1$, and the upper limit of integration is equal to infinity, we find that the input impedance of the square emitter is expressed by formula (17). Thus, the input impedances of the square and round emitters of large size are equal, if their areas are equal. If the square emitter is small, then $u_2 = u_3 = k^2 a^2 / 2\pi^2$.

Consequently, all the conclusions drawn above in relation to the input impedance of the round emitter are also correct for the square emitter of the same area. We now hypothesize that the square emitter is divided into a certain number of rectangular elements with correlation of the sides c/d , arranged, as shown in fig. 4, and connected parallel-in series. It is evident that the input impedance of the element is c/d -times larger than the input impedance of the emitter.

If the element has a square shape, then its input impedance is the linear impedance of the emitter. Consequently, the graph in fig. 3 yields not only the input impedance of the emitter, but also its linear impedance, and also in a certain scale, the input impedance of the element in the grid of assigned finite dimensions (with uniform distribution of the current over the emitter).

As shown by numerical calculation from formula (13), in a large grid of a one-sided emitter with current distribution diminishing towards the edges of the type (19), the reactive impedance of the element is comparatively small. At the same time, the active impedance of the element in this grid is almost constant and close to 120π .

This result coincides with that obtained in [3] with the help of the concept of a unified cell. It indicates the basic possibility of broad-band matching of elements in large emitters. We note that by changing the c/d ratio, there is a possibility of matching the average input resistance of the emitter elements with feeder of any assigned wave impedance W . Thus, for example, with $\epsilon_2=1$, $W=75 \text{ Ohm}$ and one-sided emission, the correlation $c/d=5$ is necessary.

With the help of this method of matching the elements of the emitter through selecting the distances between them, in certain cases one can probably obtain wider-band matching than with the help of the usually employed method using transforming properties of the elements themselves.

Efficiency of the Emitter Placed Near the Interface

We will find the efficiency of the emitter that is placed on the interface of two media. An approximate expression for the input impedance of a large-sized emitter was determined by formula (17). With the help of (12), by finding the impedance of the radiation under the same assumptions, and by using (8), we obtain the efficiency of the large-sized emitter

$$\eta = \frac{V_{\epsilon_1}}{V_{\epsilon_1} + V_{\epsilon_2}} \quad (25)$$

The impedance of radiation of a small emitter is found with the same assumptions that were made in deriving (18). By substituting

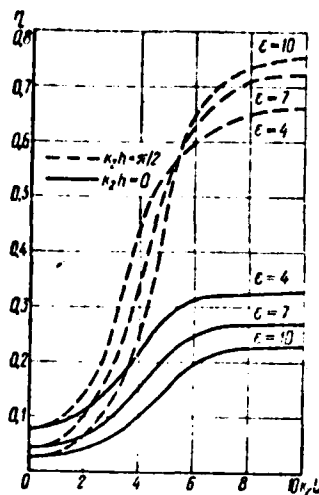


Figure 5.

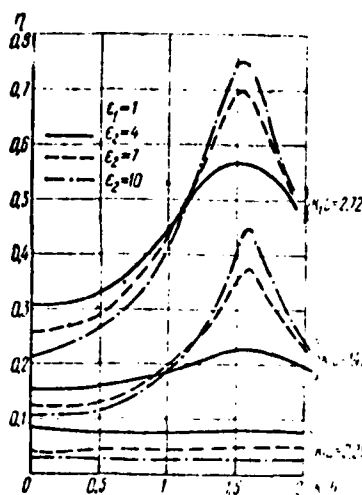


Figure 6.

in (8), we find the efficiency of the small-sized emitter

$$\eta = \frac{\sqrt{\epsilon_1}}{\epsilon_2(1 + \sqrt{\epsilon_1})} \quad (26)$$

Figure 5 shows by solid lines the dependences of efficiency on disk radius for media with different parameters that were obtained through numerical integration of accurate expressions (12) and (13). It is apparent from the presented curves that formula (25) yields satisfactory accuracy with $k_2L > 10$. On the other hand, formula (26) yields fairly accurate results if $k_2L < 0.5$.

The curves in fig. 5 determine the maximum attainable values of efficiency for an emitter of assigned parameters located on the interface if medium 2 does not have losses. It is natural that when there are losses in medium 2, the efficiency values will be lower than those shown in fig. 5. We will dwell on the dependence of efficiency on the depth of submersion of the emitter. Figure 6 presents the dependences of efficiency of disk emitters of varying radius on the depth of submersion for a medium without losses. They are found by numerical integration of (12) and (13). As is apparent from fig. 6, for large-sized emitters ($k_2L > 6$), a drastic peak appears in the dependence of efficiency on depth. Its maximum corresponds to the equality $2k_2h = \pi$.

For small-sized emitters, this peak is almost not pronounced. Figure 5 shows through the dotted lines the numerically found dependences of efficiency with optimal deepening on the disk radius. Comparison of them with the dependences of efficiency with zero deepening shows that the proper selection of emitter deepening can produce a considerable increase in the efficiency for a disk of sufficient radius ($k_2 L < 6$). It can be shown that the maximum efficiency which can thus be obtained

$$\eta = \frac{\sqrt{\epsilon_2}}{1 + \sqrt{\epsilon_2}} \quad (27)$$

Practical realization of this effect is difficult, first of all because, as is apparent from fig. 6, with an increase in permeability ϵ_2 , the width of the peak rapidly contracts, and secondly, because, as shown by the numerical calculations from formulas (12) and (13), the effect disappears when the imaginary part becomes commensurate with the real part.

Conclusion

The averaged input impedance of square ($c/d=1$) elements of the emitter which are connected on an in series-parallel circuit where the emitter radius exceeds two wavelengths in a low-conducting medium, is purely active and equal to the wave impedance of the medium with one-sided emission and half of the wave impedance of a medium with two-sided emission.

The input impedance of the emitter which is located parallel to the interface of two low-conducting media, with a change in the distance from it to the interface, changes in limits from the quantity of wave impedance of the medium with great permeability to half of this value.

The efficiency of an emitter located on the boundary of two low-conducting media whose radius exceeds one wavelength in the medium with lower permeability, is approximately proportional to the root of the ratio of dielectric permeabilities of the media.

The efficiency of the same emitter, if its radius is less than one-sixth of a wave in the medium with greater permeability, is

approximately proportional to the ratio of dielectric permeabilities of the media in the degree $3/2$.

With deepening of the emitters of sufficiently large radius, one can obtain efficiency in the low-conducting medium which is almost equal to a unit.

In conclusion, I consider it my duty to thank Professor B. V. Braude and Professor G. A. Lavrov for valuable criticism which stimulated the publication of this article.

Appendix

The system of orthogonal functions (5) can be the solution to the vector wave equation in cylindrical coordinates, if by r , φ , and z we mean the coordinates of the observation point. The projections of the vectors of the electric and magnetic fields on the φ axis in the region between the interface and the plane passing above the sources can be written with the help of these functions as follows:

$$H_{1\varphi} = \frac{\kappa_2}{i2} \sum_{n=-\infty}^{\infty} \int_0^{\infty} \{ (A_{3n\varphi}^+ + \alpha_2 A_{3n\varphi}^-) f_{2n}^+ + (A_{2n\varphi}^+ + \alpha_3 A_{2n\varphi}^-) f_{3n}^- \} \frac{l}{m_2} dl, \quad (28)$$

$$E_{1\varphi} = \frac{\mu_0 \omega}{2} \sum_{n=-\infty}^{\infty} \int_0^{\infty} \{ (A_{2n\varphi}^+ + \alpha_2 A_{2n\varphi}^-) f_{2n}^+ + (A_{3n\varphi}^+ + \alpha_3 A_{3n\varphi}^-) f_{3n}^- \} \frac{l}{m_2} dl.$$

The projections on the r axis are written analogously by replacing the φ signs by r . The flux of Poynting's vector passing upwards through the plane $z=z_1$,

$$P_1(z) = \int_0^{2\pi} \int_0^{\infty} (H_{1\varphi} E_{1r}^* - H_{1r} E_{1\varphi}^*)|_{z=z_1} r dr d\varphi. \quad (29)$$

By substituting (28) and by using the conditions for orthogonality, we obtain

$$\int_0^{2\pi} A_{3n\varphi}^+ A_{3n'\varphi}^{+*} d\varphi = 0 \quad (n \neq n'),$$

$$\int_0^{2\pi} A_{2n\varphi}^+ A_{2n'\varphi}^{+*} d\varphi = 0 \quad (n \neq n'), \quad (30)$$

$$\int_0^{2\pi} \int_0^{\infty} \int_0^{\infty} A_{3nr}^+(l) A_{3nr'}^{+*}(l') l' dl' r dr d\varphi = 2\pi l^2 e^{-22Jm\eta_2 l},$$

$$\int_0^{2\pi} \int_0^{\infty} \int_0^{\infty} A_{2nr}^+(l) A_{2nr'}^{+*}(l') l' dl' r dr d\varphi = 2\pi l^2 e^{-22Jm\eta_2 l},$$

as well as the obvious correlations:

$$\begin{aligned} \frac{\Lambda_z(\mu, \omega)}{4} &= \frac{30\pi \kappa_2^2}{\sqrt{\epsilon_2}}, \quad A_{3n\varphi} = -A_{3n\varphi} e^{-12m_2 z}, \\ A_{3nr}^- &= -A_{3nr}^+ e^{-12m_2 z}, \quad A_{3n\varphi}^+ = \frac{i m_2}{\kappa_2} A_{2nr}^+, \\ A_{3nr}^+ &= -\frac{i m_2}{\kappa_2} A_{2n\varphi}^+, \end{aligned} \quad (31)$$

after simple transforms, we obtain (1). The field in the region that lies below the plane which places below the sources is written as:

$$\begin{aligned} H_{2\varphi} &= \frac{\kappa_2}{i2} \sum_{n=-\infty}^{\infty} \int_0^{\infty} [(f_{3n}^- + \alpha_3 f_{3n}^+) A_{2n}^- + (f_{2n}^- + \alpha_2 f_{2n}^+) A_{3n}^-] \frac{l}{m_2} dl, \\ E_{2\varphi} &= \frac{\mu_0 \omega}{2} \sum_{n=-\infty}^{\infty} \int_0^{\infty} [(f_{2n}^- + \alpha_2 f_{2n}^+) A_{2n}^- + (f_{3n}^- + \alpha_3 f_{3n}^+) A_{3n}^-] \frac{l}{m_2} dl. \end{aligned} \quad (32)$$

The projections on the r axis are written analogously through replacement in (32) of the signs φ by r . By substituting (32) into the expression for the flux of Poynting's vector which passes downwards through the plane $z=z_2$

$$P_2(z) = \int_0^{2\pi} \int_0^{\infty} (H_{2r} E_{2\varphi}^* - H_{2\varphi} E_{2r}^*)|_{z=z_2} r dr d\varphi \quad (33)$$

and by using (3) and (31), we obtain (2).

Bibliography

1. Braude, B. V. "Method of Computing the Complete Active Impedance of an Antenna with Regard for the Finite Conductance of the Earth," Radiotekhnika, Vol. 1, No. 5, 1946.
2. Kul'tsep, V. P. "Input Impedance of a System Made of Intersecting Low-Arranged Vibrators," Antenny ["Antennas"], Collection of articles edited by A. A. Pistol'kors, No. 6, 1969.
3. Skanirovushchiye antennoye sistemy SVCh ["Scanning Antennas of the SHF System"], Trans. from Eng., Moscow, Sovetskoye radio, 1966.

ANALYSIS OF THE PROPERTIES OF CONNECTED
VIBRATOR STRUCTURES

N. A. Bey and N. M. Yakusheva

Summary

The task of determining the phase velocities of the main waves propagating in connected infinite vibrator structures is solved by the method of integrated equations. The obtained correlations make it possible to link the phase velocities of the main waves with the geometric parameters of the system.

Introduction

Small transverse dimensions, small connection in the opposite direction, and the possibility of forming a sector beam pattern are the advantages of antennas of axial radiation, and in particular, director antennas when they are used in phased antenna arrays. In order to solve the task of synthesizing the beam pattern of the emitter for a director-type antenna which operates in an array, it is necessary to know the size of the linear coupling coefficient. Its determination is reduced to calculation of the phase velocities of the even and odd waves.

It should be noted that in publication [1] which also covers an analysis of the properties of the connected vibrator structures, the obtained correlations are very cumbersome, and only the properties of the structures arranged in the H-plane with equal geometric parameters are numerically analyzed.

Derivations of the Main Correlations

We will examine a general case of connected structures which are arranged along the x-axis and are shifted along the y and z axes to distances a_y and a_z (fig. 1). We will consider the vibrators to be ideally conducting thin tubes, and $d/l \ll 1$ and $d/a \ll 1$. The boundary condition will be the equality of the tangential field components on the vibrator surface to zero. As the conditions for infinit y, we will use the condition of maximum absorption. Assume that all the vibrators are excited with a linear change in phase such that qa_x --phase shift between neighboring vibrators $\left(-\frac{\pi}{a_x} < q < \frac{\pi}{a_x}\right)$:

$$K_n(z) = K_{01}(z) \exp(i q a_1 n)$$

$$K_m(z) = K_{02}(z) \exp(i q a_2 m).$$

where n and m--numbers of vibrators of first and second channels.

We will introduce the cylindrical system of coordinates z, r, ϕ with beginning in the center of the zero vibrator of the first channel. By using the expression obtained in [2] for the vector potential near the surface of the zero vibrator of the first channel, and the boundary condition, after certain transforms we obtain the integrodifferential equation for the current of the first channel vibrator

$$\begin{aligned} \frac{\partial^2 J_1}{\partial z_1^2} + \kappa^2 J_1 = \frac{i 4 \pi \kappa}{W} \left[K_1(z) + \frac{W}{i 4 \pi a_1} \sum_{n=-\infty}^{\infty} \int_{-\infty}^{\infty} dt \times \right. \\ \times \frac{(1-\rho) \int_{-l_1}^{+l_1} dz'_1 J'_1(z'_1)}{i \sqrt{f_1}} \frac{\exp[i \kappa l (z_1 - z'_1)]}{l_1} + \frac{W \kappa}{4 \pi a_2} \sum_{m=-\infty}^{\infty} \int_{-\infty}^{\infty} dt \times \\ \times \left. \frac{\int_{-l_2}^{+l_2} dz'_2 J'_2(z'_2) \exp[i \kappa \sqrt{f_2} (y_1 - a_y - y'_2) + i \kappa l (z_1 + a_z - z'_2)]}{\sqrt{f_2}} \right]. \end{aligned}$$

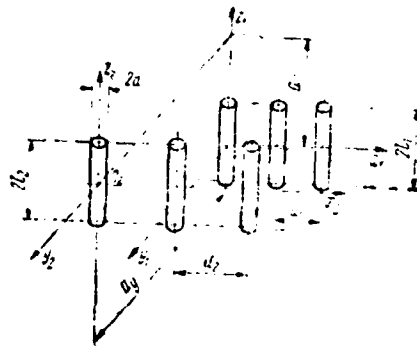


Figure 1.

Here: $\kappa = \frac{2\pi}{\lambda}$; $\chi = \frac{1}{2 \ln(\kappa d)}$; $\beta = \frac{v_\phi}{c}$;

$$f_{1,2} = 1 - \rho - \left(\frac{1}{\beta} + \frac{s\lambda}{a_{1,2}} \right)^2; s = n \text{ for } f_1 \text{ and } m \text{ for } f_2.$$

The boundary condition has the appearance $J_{1,2}(\pm l_{1,2}) = 0$.

Analogously, an equation is written for the current of the second channel vibrator.

In [2], the integrodifferential equation for the vibrator currents is solved on the assumption that the lengths of the vibrators differ little from the resonance $(|\kappa l_{1,2} - n \frac{\pi}{2}| \leq 1)$. Here we will examine

the solution for the case where detuning of the vibrators is great, i.e., $|\kappa l_{1,2} - \frac{\pi}{2}| \gg |\chi|$. In a similar way as was done in publication [3],

we will use the method of perturbations, and we will look for a solution in the form of a power series $J_{1,2} = J_{0,1,2} + \chi J_{1,1,2} + \chi^2 J_{2,1,2} + \dots$ (η -- number

of channel that the vibrator belongs to).

By substituting this series in equation (1) and the boundary conditions, we obtain a system of differential equations with boundary conditions. The solution to the first equation will be $J_{012}(z) = 0$.

The task is further reduced to solving the system of equations:

$$\left. \begin{aligned} J_{11}'(z_1) + \kappa^2 J_{11}(z_1) &= \frac{i 4\pi \kappa}{W} K_1(z), \quad J_{11}(\pm l_1) = 0 \\ J_{21}'(z_1) + \kappa^2 J_{21}(z_1) &= \frac{i 4\pi \kappa}{W} [G_{11q}(J_1, z) + G_{21q}(J_1 z)], \quad J_{21}(\pm l_1) = 0 \end{aligned} \right\}, \quad (2)$$

$$\left. \begin{aligned} J_{12}'(z_2) + \kappa^2 J_{12}(z_2) &= \frac{i 4\pi \kappa}{W} K_2(z); \quad J_{12}(\pm l_2) = 0 \\ J_{22}'(z_2) + \kappa^2 J_{22}(z_2) &= \frac{i 4\pi \kappa}{W} [G_{22q}(J_1, z) + G_{12q}(J_1, z)], \quad J_{22}(\pm l_2) = 0 \end{aligned} \right\}. \quad (3)$$

The solution to the first equations in systems (2) and (3) obtained in publication [3] for the case where the outside emf is concentrated in the middle of the vibrator $|K(z) = U\delta(z)|$, looks like

$$J_1(z') = U \frac{i 2\pi}{W} [\sin(\kappa|z'|) - \operatorname{tg}(\kappa l) \cos(\kappa z')].$$

We will determine $G_{11, 22q}(J_1, z)$ and $G_{21, 12}(J_1, z)$:

$$\begin{aligned} G_{11, 22q}(J_1, z) &= -\frac{i W}{4\pi a_{1,2}} \sum_{n, m=-\infty}^{\infty} \int_{-\infty}^{\infty} dt \frac{(1-t^2)}{t \sqrt{f_{1,2}}} \left\{ \lim_{\epsilon \rightarrow 0} \int_{-l_{1,2}}^{-\epsilon} \times \right. \\ &\quad \times [\sin(\kappa|z'|) - \operatorname{tg}(\kappa l_{1,2}) \cos(\kappa z')] dz'_{1,2} + \lim_{\epsilon \rightarrow 0} \int_{\epsilon}^{l_{1,2}} [\sin(\kappa|z'|) - \\ &\quad \left. - \operatorname{tg}(\kappa l_{1,2}) \cos(\kappa z')] dz'_{1,2} \right\} \exp[i \kappa l (z_{1,2} - z'_{2,1})] = \\ &= -\frac{W}{2\pi a_{1,2}} \sum_{n, m=-\infty}^{\infty} \int_{-\infty}^{\infty} dt \frac{\exp(i \kappa z)}{V f_{1,2}} \left[1 - \frac{\cos(\kappa l_{1,2})}{\cos(\kappa l_{1,2})} \right], \\ G_{12, 21q}(J_1 z) &= \frac{W}{2\pi a_{1,2}} \sum_{n, m=-\infty}^{\infty} \int_{-\infty}^{\infty} dt \frac{\exp(i \kappa z) \cos(\kappa a_{1,2})}{V f_{1,2} \exp(a_{1,2} \kappa - l_{1,2})} \times \\ &\quad \times \left[1 - \frac{\cos(\kappa l_{1,2})}{\cos(\kappa l_{1,2})} \right]. \end{aligned}$$

The solution to the second equations of systems (2) and (3) is sought in the form

$$J_{21,2q}(z_{1,2}) = C_1 \cos(\kappa z) - C_2 \sin(\kappa z) + \frac{U + 4\pi}{W a_{1,2} \kappa} \sum_{n, m=-\infty}^{\infty} \int_{-\infty}^{\infty} dt \times \\ \times \frac{\exp(i \kappa t)}{(1-t^2) \sqrt{-f_{1,2}}} \left[1 - \frac{\cos(\kappa l_{1,2})}{\cos(\kappa l_{1,2})} \right] \left[1 + \frac{\cos(\kappa a_2 t)}{\exp(a_y \kappa \sqrt{-f_{1,2}})} \right]$$

With regard for the boundary conditions, we obtain:

$$C_1 = -\frac{U + 4\pi}{W a_{1,2} \kappa} \sum_{n, m=-\infty}^{\infty} \int_{-\infty}^{\infty} dt \frac{\left[1 - \frac{\cos(\kappa l_{1,2})}{\cos(\kappa l_{1,2})} \right]}{(1-t^2) \sqrt{-f_{1,2}}} \times \\ \times \left[1 + \frac{\cos(\kappa a_2 t)}{\exp(a_y \kappa \sqrt{-f_{1,2}})} \right] \frac{\cos(\kappa l_{1,2})}{\cos(\kappa l_{1,2})}, \\ C_2 = \frac{U + 4\pi}{W a_{1,2} \kappa} \sum_{n, m=-\infty}^{\infty} \int_{-\infty}^{\infty} dt \frac{\left[1 - \frac{\cos(\kappa l_{1,2})}{\cos(\kappa l_{1,2})} \right]}{(1-t^2) \sqrt{-f_{1,2}}} \times \\ \times \left[1 + \frac{\cos(\kappa a_2 t)}{\exp(a_y \kappa \sqrt{-f_{1,2}})} \right] \frac{\sin(\kappa l_{1,2})}{\sin(\kappa l_{1,2})}.$$

After transforms, (4) acquires the appearance

$$J_{21,2q}(z_{1,2}) = \frac{-i 4\pi U}{W a_{1,2} \kappa} \sum_{n, m=-\infty}^{\infty} \int_{-\infty}^{\infty} dt \frac{\left[1 - \frac{\cos(\kappa l_{1,2})}{\cos(\kappa l_{1,2})} \right]}{(1-t^2) \sqrt{-f_{1,2}}} \times \\ \times \left[1 + \frac{\cos(\kappa a_2 t)}{\exp(a_y \kappa \sqrt{-f_{1,2}})} \right] \frac{\cos(\kappa l_{1,2})}{\cos(\kappa l_{1,2})} \cos(\kappa z) + \\ + \frac{U + 4\pi}{W a_{1,2} \kappa} \sum_{n, m=-\infty}^{\infty} \int_{-\infty}^{\infty} dt \frac{1}{(1-t^2) \sqrt{-f_{1,2}}} \left[1 - \frac{\cos(\kappa l_{1,2})}{\cos(\kappa l_{1,2})} \right] \times \\ \times \left[1 + \frac{\cos(\kappa a_2 t)}{\exp(a_y \kappa \sqrt{-f_{1,2}})} \right] \frac{\sin(\kappa l_{1,2})}{\sin(\kappa l_{1,2})} \sin(\kappa z) + \\ + \frac{U + 4\pi}{W a_{1,2} \kappa} \sum_{n, m=-\infty}^{\infty} \int_{-\infty}^{\infty} dt \frac{\cos(\kappa l_{1,2}) \left[1 - \frac{\cos(\kappa l_{1,2})}{\cos(\kappa l_{1,2})} \right]}{(1-t^2) \sqrt{-f_{1,2}}} \times \rightarrow \\ \rightarrow \times \left[1 + \frac{\cos(\kappa a_2 t)}{\exp(a_y \kappa \sqrt{-f_{1,2}})} \right].$$

At the point $z=0$:

$$J_{11,2q}(0) = -\frac{U i 2\pi}{W} \operatorname{tg}(\kappa l_{1,2}),$$

$$J_{21,2q}(0) = \frac{U i 4\pi}{W a_{1,2} \kappa} \sum_{n, m=-\infty}^{\infty} \int_{-\infty}^{\infty} dt \frac{\left[1 - \frac{\cos(\kappa l_{1,2})}{\cos(\kappa l_{1,2})}\right]^2}{(1-t^2) \sqrt{-f_{1,2}}} \times$$

$$\left[1 + \frac{\cos(\kappa a_2 t)}{\exp(a_y \kappa \sqrt{-f_{1,2}})}\right]. \quad (5)$$

The solution to (2) and (3) is written in the form

$$J_{1,2} = \gamma J_{11,2} + \gamma^2 J_{21,2}. \quad (6)$$

After substituting (5) into (6), we obtain

$$J_{1,2q} = U \left\{ -\frac{i 2\pi \gamma}{W} \operatorname{tg}(\kappa l_{1,2}) + \frac{i 4\pi \gamma^2}{W a_{1,2} \kappa} \times \right.$$

$$\times \sum_{n, m=-\infty}^{\infty} \int_{-\infty}^{\infty} dt \frac{\left[1 - \frac{\cos(\kappa l_{1,2})}{\cos(\kappa l_{1,2})}\right]^2 \left[1 + \frac{\cos(\kappa a_2 t)}{\exp(a_y \kappa \sqrt{-f_{1,2}})}\right]}{(1-t^2) \sqrt{-f_{1,2}}} \Bigg\}.$$

In a similar manner as was done in [4], we find the equation which links the phase velocities of the main waves which are propagated in the system with its geometric parameters (with accuracy to terms on the order of χ^2):

$$-\operatorname{tg}(\kappa l_{1,2}) + \frac{2\gamma}{a_{1,2} \kappa} \sum_{n, m=-\infty}^{\infty} \int_{-\infty}^{\infty} dt \frac{\left[1 - \frac{\cos(\kappa l_{1,2})}{\cos(\kappa l_{1,2})}\right]^2}{(1-t^2) \sqrt{-f_{1,2}}} \times$$

$$\times \left[1 + \frac{\cos(\kappa a_2 t)}{\exp(a_y \kappa \sqrt{-f_{1,2}})}\right] = 0. \quad (7)$$

In particular, for a single structure, (7) acquires the appearance

$$-\operatorname{tg}(\kappa l_{1,2}) + \frac{2\gamma}{a \kappa} \sum_{n, m=-\infty}^{\infty} \int_{-\infty}^{\infty} dt \frac{\left[1 - \frac{\cos(\kappa l_{1,2})}{\cos(\kappa l_{1,2})}\right]^2}{(1-t^2) \sqrt{-f_{1,2}}} = 0. \quad (8)$$

Results of Numerical Calculation

Figure 2 gives the relationship (curve 1) computed according to formula (8), and for comparison, the relationship taken from [1] (curve 2) which also characterizes a single structure. Figure 3 presents the

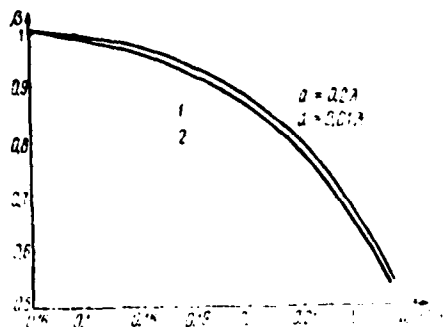


Figure 2

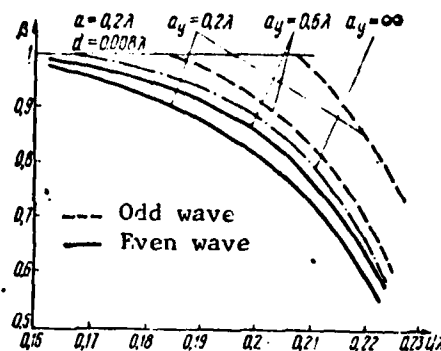


Figure 3

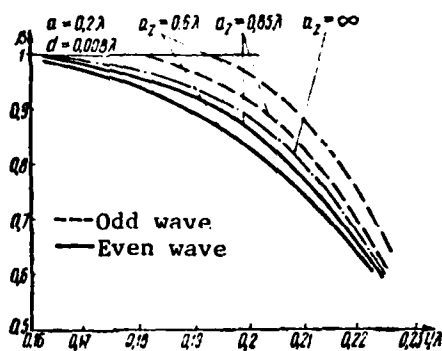


Figure 4.

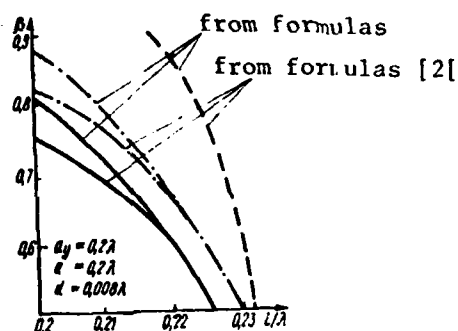


Figure 5.

curves $\beta=f(1/\lambda)$ of even and odd waves which propagate in the connected structures with the same geometric parameters, arranged in the H-plane. Figure 4 presents analogous curves for structures in the E-plane. Fig. 5 presents the results of computing the relationship $\beta=f(1/\lambda)$ for even (solid line) and odd (dotted line) waves in connected structures, and for the main wave of a single structure (dot-dash line). As is apparent from fig. 5, the results of the calculation from the formulas for the systems made of slightly detuned vibrators [2] satisfactorily coincide with the results of calculations according to formulas (7) and (8) only for $1 > (0.215-0.220)\lambda$.

Bibliography

1. Mailloux, R. Trans. IEEE, Vol. AP-13, No. 4, 1965, pp. 499-507.

2. Bey, N. A.; and Ryakusheva, N. M. Radiotekhnika, Vol. 26, No. 11, 1971, pp. 84-86.
3. Leontovich, M. A.; and Levin, M. L. ZhTF, Vol. 14, No. 9, 1944, pp. 481-506.
4. Baklanov, Ye. V. Radiotekhnika i elektronika, Vol. 13, No. 2, 1968, pp. 204-211.

ASSESSMENT OF AIRCRAFT CAPACITIVE CIRCUIT
MEDIUM WAVE ANTENNAS ACCORDING TO THEIR EFFICIENCY

E. O. Brudnyy and L. Ya. Il'nitskiy

Summary

This work presents a method for assessing aircraft capacitive circuit medium wave antennas according to their efficiency.

The measure of efficiency is the product of the antenna capacitance times the active altitude. An expression is obtained which links the antenna efficiency to its geometric dimensions.

The suggested method produces the optimal dimensions for aircraft capacitive circuit antennas direction during their designing.

Capacitive circuit antennas are currently used as nondirectional antennas of aircraft medium-wave range radio compasses. However, definite difficulties arise in designing these antennas in the selection of the optimal geometric dimensions of the vertical and horizontal circuit arms. These difficulties are due to the lack of criteria for assessing the operating quality of the circuit antenna associated with its geometric dimensions.

This article presents a method for assessing the capacitive circuit antennas according to their efficiency. By using the quasi-static principle to analyze the operation of the circuit antenna of medium waves [1-3], one can draw the conclusion that the main measure of its efficiency is the product of antenna capacitance times the active length. It is quite obvious that the voltage at the outlet of the radio compass receiver will be proportional to this product.

The antenna efficiency is tied to the geometric dimensions in a quite definite manner.

Aircraft construction usually uses a circuit antenna which consists of a metal tube (or conductor) which is fastened to the fuselage with the help of insulation struts and closed by a dielectric cone. The complete capacitance of this antenna can be determined from formula [3]

$$C_A = \frac{24.13(l+h)}{\lg \left\{ \frac{2h}{d} \left[1 + \sqrt{1 - \left(\frac{d}{2h} \right)^2} \right] \right\}}, \text{ pf} \quad (1)$$

where l --length of horizontal circuit arm, m, h --length of vertical circuit arm, m d --diameter of tube (conductor) of which the circuit is made, m.

In practice, in designing the aircraft antennas of this type, the condition $2h \gg d$ is always fulfilled, and formula (1) can be simplified

$$C_A \approx \frac{24.13(l+h)}{\lg \frac{4h}{d}}, \text{ pf} \quad (2)$$

It should be noted that the real capacitance of the antenna must somewhat exceed that calculated in formula (2), since here the calcula-

tion does not consider the continuous insulator which increases the total capacitance of the circuit.

Because the examined antenna operates in the range of medium waves, one can consider the distribution of current on the vertical circuit arm to be uniform. However, this conclusion is only correct with a definite correlation between the lengths of the horizontal and vertical antenna arms.

We will designate through h_{H0} the active height of the circuit antenna which is installed above the flat counterweight, then [6]

$$h_{\text{H0}} = \frac{1}{I_0} \int_0^l I(z) dz, \quad (3)$$

where I_0 --current in the antenna base, $I(z)$ --distribution function of the current along the antenna.

Assuming that the horizontal and vertical antenna arms are made of wire of equal diameter, and that the following condition is fulfilled in the entire working range of the antenna

$$\lambda_{\text{раб}} > 2\lambda_0,$$

where $\lambda_{\text{раб}}$ --length of working wave of antenna, λ_0 --natural length of antenna wave; expression (3) can be written in the form:

$$h_{\text{H0}} \approx h \left(1 - \frac{h\kappa}{2 \left[\kappa h + \text{arctg} \left(\frac{W_h}{W_l} \text{tg } \kappa l \right) \right]} \right), \quad \mu, \quad (4)$$

where W_h --wave impedance of vertical circuit arm,
 W_l --wave impedance of horizontal circuit arm, $\kappa = \frac{2\pi}{\lambda}$.

It follows from an analysis of formula (4) that when the condition is fulfilled

$$l > 6h$$

with accuracy sufficient for practice, one can consider that

$$h_{\text{H0}} \approx h. \quad (5)$$

For design considerations, the height of the aircraft circuit antenna is usually limited by the condition:

$$h \leq 0,15 \mu,$$

then the equality (5) will be correct for the antennas where

$$l \geq 0.9 \div 1.0 \text{ m.}$$

Taking into consideration that expression (5) is correct only for an antenna installed above the flat counterweight, we will introduce into the examination h_A --the active height of the circuit antenna with regard for the effect of the aircraft fuselage, which is approximated by the surface of an infinite round cylinder.

It is known from publication [4] that

$$h_A = k_y h_{A0}, \text{ m.} \quad (6)$$

where k_y --dimensionless coefficient of antenna elongation.

For the circuit antennas, k_y depends on l , increasing proportionally to the length of the horizontal antenna arm. Thus, for example, for an antenna with horizontal arm $l=1$ m, the coefficient of elongation will equal 2, for an antenna with horizontal arm $l=2$ m, the coefficient of elongation will equal 2.5, and for an antenna with $l=3$ m, $k_y=3$ [3].

It follows from expressions (2) and (6) that

$$S \approx \frac{24.13 k_y h (l + h)}{\lg \frac{4h}{d}}, \text{ pf} \cdot \text{m}, \quad (7)$$

where S --efficiency of circuit antenna.

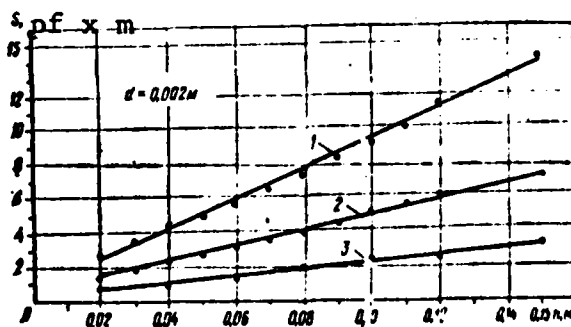


Figure 1.

Figures 1-4 present graphs for the efficiency of aircraft circuit antennas for different values of their design dimensions. The

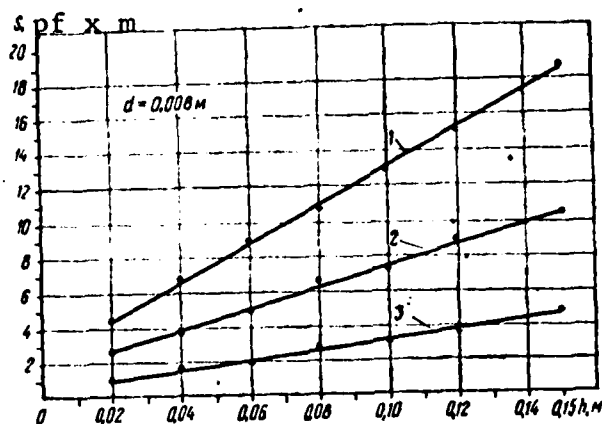


Figure 2.

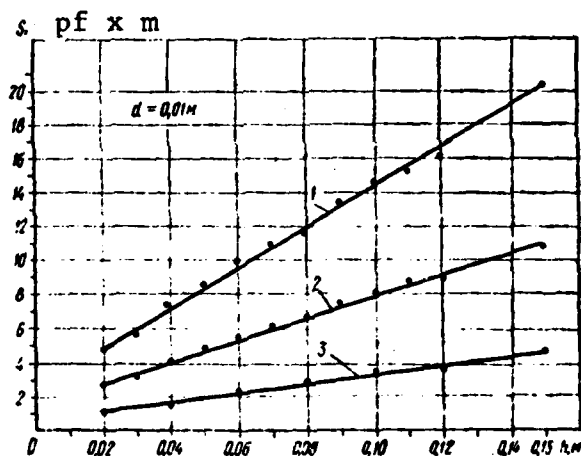


Figure 3.

relationships (with $h \ll \lambda$) expressed by straight lines 1, are computed for the circuits with length of the horizontal arm $l=3$ m, straight lines 2, for circuits with $l=2$ m, and straight lines 3, for circuits with $l=1$ m. The graph calculations were made according to formula (7).

If the minimum value of efficiency of the circuit antenna is assigned based on the conditions to guarantee normal operation of the radio compass (or other reception device that the antenna must operate with), then from the graphs of figs. 1-4 one can easily determine the geometric dimensions of the circuit which are necessary for this.

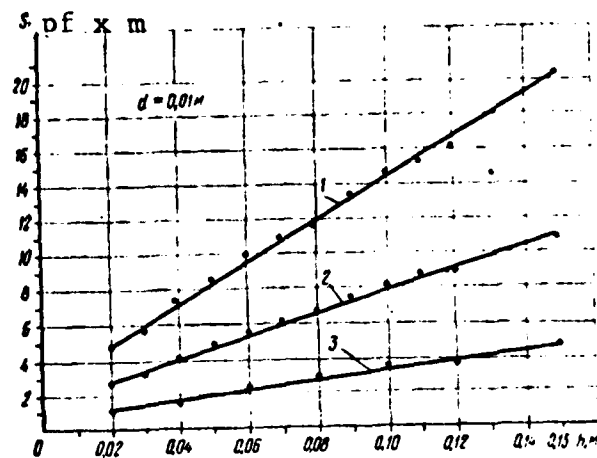


Figure 4.

The suggested method was experimentally verified [5]. The experiment was conducted with a capacitive circuit antenna installed on the AN-24 aircraft, and had geometric dimensions ($h=0.01$ m; $l=3.6$ m, $d=0.007$). The measurements of the electric parameters of this antenna yielded the following values ($h_a \approx 0.28$ m and $C_A \approx 76$ pf, consequently, $S \approx 21.3$ pf x m). The minimum efficiency of the antenna that was necessary for the normal operation of the radio compass was selected as equal to 6 pf m. Then, from the graph 1 in fig. 3, it was determined that the antenna with parameters $h=0.01$ m, $l=2$ m and $d=0.007$ m must guarantee the assigned efficiency. After shortening the horizontal arm of the antenna to 2 m, the measurements of the electric parameters of the antenna yielded the following results: $h_a \approx 0.23$ m and $C_a \approx 30$ pf.

Thus, the real efficiency of the antenna became equal to 6.9 pf m, while that obtained from the graph in fig. 3, 7 pf m. Decrease in antenna efficiency did not affect the operating quality of the radio compass, while the weight and overall dimensions of the circuit were considerably reduced [6],

Taking into account that the suggested method makes it possible to obtain the optimal dimensions of the aircraft capacitive medium wave circuit antennas directly during their designing, one can hope that it will be widely employed.

Bibliography

1. Granger, J. V.; and Bolljahn, J. T. "Aircraft Antennas," Proc. JRE, Vol. 43, May, No. 5, 1955, pp 533-550.
2. Booljahn, J. T. "Electrically Small Antennas and the Low-Frequency Aircraft Antenna Problem," Trans. of JRE, Vol. AP-1, Oct. No. 2, 1953, pp. 46-56.
3. Reznikov, G. B. Samoletnyye antennoy srednikh i korotkikh voln ["Medium and Short-Wave Aircraft Antennas"], KVIAPU, 1958.
4. Weissfloch, A.; and Ancona, C. "Utilisation de la Cage Electrostatique pour L'etude de Certaines Antennas D'avion," L'onde Electrique, Vol. 37, No. 363, 1957, pp. 599-604.
5. Brudnyy, E. O. Issledovaniye nekotorykh metodov povysheniya tochnosti samoletnykh radiokompasov ["Study of Certain Methods to Improve the Accuracy of Aircraft Radio Compasses"], Dissertation, KNIGA, 1970.
6. Pistol'kors, A. A. Antennoy ["Antennas"], Moscow, Sosizdat literatury po voprosam svyazi i radio, 1947.

END

DATE
FILMED

1-82

DTIC